

NEUTRINO PROPERTIES BEFORE AND AFTER KAMLAND

S PAKVASA* AND J W F VALLE†

**Department of Physics and Astronomy, University of Hawaii, Manoa 2505 Correa Road, Honolulu, Hawaii 96822 (USA)*

† *Instituto de Física Corpuscular C.S.I.C. Universitat de València Edificio Institutos de Paterna, Apt 22085, E-46071 València (Spain)*

(Received 17 January 2003; Accepted 30 June 2003)

We review neutrino oscillation physics, including the determination of mass splittings and mixings from current solar, atmospheric, reactor and accelerator neutrino data. A brief discussion is given of cosmological and astrophysical implications. Non-oscillation phenomena such as neutrinoless double beta decay would, if discovered, probe the absolute scale of neutrino mass and also reveal their Majorana nature. Non-oscillation descriptions in terms of spin-flavour precession (SFP) and non-standard neutrino interactions (NSI) currently provide an excellent fit of the solar data. However they are at odds with the first results from the KamLAND experiment which imply that, despite their theoretical interest, non-standard mechanisms can only play a sub-leading role in the solar neutrino anomaly. Accepting the LMA-MSW solution, one can use the current solar neutrino data to place important restrictions on non-standard neutrino properties, such as neutrino magnetic moments. Both solar and atmospheric neutrino data can also be used to place constraints on neutrino instability as well as the more exotic possibility of *CPT* and Lorentz Violation. We illustrate the potential of future data from experiments such as KamLAND, Borexino and the upcoming neutrino factories in constraining non-standard neutrino properties.

Key Words: Standard Neutrino Oscillations; Spin Flavour Precision; Non Standard Neutrino Interactions; Neutrino Magnetic Moments; *CPT* and Lorentz Violation; Neutrino Decay; Neutrino Mixing in Cosmology

1 Introduction

Since the early Davis experiment using the geochemical method to detect solar neutrinos via the $\nu_e + {}^{37}\text{Cl} \rightarrow {}^{37}\text{Ar} + e^-$ reaction at Homestake¹, solar neutrino research has gone a long way to become now a mature field. The subsequent Gallex², Sage³ and GNO⁴ experiments have not only confirmed the consistency of the basic elements of solar energy generation, but also established that the deficit seen in the chlorine experiment also exists⁴ in the reaction $\nu_e + {}^{71}\text{Ga} \rightarrow {}^{71}\text{Ge} + e^-$. Direct detection with Cerenkov techniques using $\nu_e e$ scattering on water at Super-K⁵, and heavy water at SNO^{6,7} has given a robust confirmation that the number of solar neutrinos detected in these underground experiments is less than expected from theories of energy generation in the Sun⁸. Especially relevant is the sensitivity of the SNO experiment to the neutral current (NC). Altogether these experiments provide a solid evidence for solar neutrino conversions

and, therefore, for physics beyond the Standard Model (SM). Current data indicate that the mixing angle is large⁹, the best description being given by the LMA-MSW (Mikheyev-Smirnov-Wolfenstein) solution¹⁰, already hinted at previously from the flat Super-K recoil electron spectra¹¹. We will briefly describe the results of the analysis of solar neutrino data and the resulting parameters in Sec.3.1.

Atmospheric neutrinos are produced in hadronic showers initiated by cosmic-ray collisions with air in the upper atmosphere^a. They have been observed in several experiments¹². Although individual ν_μ or ν_e fluxes are only known to within 20 – 30% accuracy, their ratio is predicted to within 5% over energies varying from 0.1 GeV to tens of GeV¹³. The long-standing discrepancy between the predicted and measured μ/e ratio of the muon-type ($\nu_\mu + \bar{\nu}_\mu$) over the e -type ($\nu_e + \bar{\nu}_e$) atmospheric neutrino fluxes, has shown up both in water Cerenkov experiments (Kamiokande, Super-K and IMB) as well as in the iron calorimeter Soudan2 experiment. In addition, a strong zenith-angle dependence has been found both in the sub-

^a See ref.[9] for an extensive list of experimental references

GeV and multi-GeV energy range, but only for μ -like events, the zenith-angle distributions for the e -like being consistent with expectation. Such zenith-angle distributions have also been recorded for upward-going muon events in Super-K and MACRO, which are also consistent with the ν_μ oscillation hypothesis. The atmospheric neutrino data analysis is summarized in Sec.3.2.

On the other hand, one has information on neutrino oscillations from reactor and accelerator data, discussed in Sec.3. Except for the LSND experiment¹⁴, which claims evidence for $\bar{\nu}_e$ appearance in a $\bar{\nu}_\mu$ beam, all of these report no evidence for oscillations. These experiments include the short baseline disappearance experiments Bugey¹⁵ and CDHS¹⁶, as well as the KARMEN neutrino experiment¹⁷.

Particularly relevant is the non-observation of oscillations at Chooz and Palo Verde reactors¹⁸, which provides an important restriction on the parameters Δm_{32}^2 and $\sin^2(2\theta_{13})$.

Turning now to the new generation of long baseline neutrino oscillation searches, in a recent paper¹⁹ KamLAND has found for the first time strong evidence for the disappearance of neutrinos travelling from a power reactor to a far detector, located at the Kamiokande site. Most of the $\bar{\nu}_e$ flux incident at KamLAND comes from plants located between 80 – 350 km from the detector, making the average baseline of about 180 kilometers, long enough to provide a sensitive probe of the LMA-MSW solution of the solar neutrino problem¹¹. Therefore these results of the KamLAND collaboration constitute the first test of the solar neutrino oscillation hypothesis with terrestrial experiments and man-produced neutrinos. KamLAND also finds the parameters describing this disappearance in terms of the oscillations to be consistent with what is required to account for the solar neutrino problem. As we will comment in Sec.9 this implies that non-standard solutions cannot be the leading explanation to the solar neutrino anomaly.

On the other hand the K2K experiment has recently observed positive indications of neutrino oscillation in a 250 km long-baseline setup²⁰. The collaboration observes a reduction of ν_μ flux together with a distortion of the energy spectrum. The probability that the observed flux at Super-K is a statistical fluctuation without neutrino oscillation is less than 1%.

2 Basic Neutrino Parameters

2.1 Neutrino Oscillation Parameters

Current neutrino data require three light neutrinos participating in the oscillations. Correspondingly, the simplest structure of the neutrino sector involves the following parameters:

- the solar angle $\theta_{\text{SOL}} \equiv \theta_{12}$ (large, but substantially non-maximal) and the solar splitting $\Delta m_{21}^2 \equiv \Delta m_{\text{SOL}}^2$
- the atmospheric angle $\theta_{\text{ATM}} \equiv \theta_{23}$ (nearly maximal) and the atmospheric splitting $\Delta m_{32}^2 \equiv \Delta m_{\text{ATM}}^2 \gg \Delta m_{\text{SOL}}^2$
- the reactor angle θ_{13} (small)

Since in the Standard Model neutrinos are massless, their masses must arise from some new physics. An attractive possibility is the seesaw mechanism^{21–23}. However nothing is presently known about whether this is the mechanism producing neutrinos masses and, if so, what is the magnitude of the corresponding mass scale. In fact a more general view is that neutrino masses come from some unknown dimension-five operator²⁴.

In contrast, neutrino masses could well be generated at the weak scale. One possibility is to have them induced by radiative corrections²⁵. Alternatively, neutrino masses may have a supersymmetric origin, resulting from the spontaneous violation of R parity²⁶. In this case one is left with a hybrid scheme²⁷ where only the atmospheric scale comes from a (weak-scale) seesaw, while the solar scale is calculable from radiative corrections^b.

Out of the three neutrino masses, only two splittings are fixed by oscillation data. As will be seen in Secs.3.1 and 3.2 the neutrino mass splittings needed to fit the observed solar and atmospheric neutrino anomalies are somewhat hierarchical. Depending on the sign of Δm_{32}^2 there are three types of neutrino mass spectra which fit current observation: quasi-degenerate^{29–31}, normal, such as typical of seesaw models and bilinear R-parity violation, and inverse-hierarchical neutrino masses.

Turning to the three mixing angles, they are a natural feature of gauge theories and follow simply as a result of the fact that in general $I=1/2$ (up-type) and

^b The idea that neutrino masses arise from broken R parity supersymmetry can be tested at collider experiments²⁸

$I=-1/2$ (down-type) Yukawa couplings (mass matrices) are not simultaneously diagonal. Typically mixing angles are not predicted from first principles, as we lack a basic theory of flavour. However there has been a flood of recent activity in trying to *post-dict* neutrino mixing angles^{30–33}.

Finally, the simplest structure of the lepton mixing matrix implied by a gauge theory of the weak interaction contains, in addition, three CP violating phases^{34, 35}.

- one Kobayashi-Maskawa-like CP phase
- two Majorana-type CP phases

The Majorana-type phases drop out from $\Delta L = 0$ processes, such as standard oscillations^{35, 36}. As for the “Dirac” CP phase, it does appear in such lepton-number conserving oscillations. However, the corresponding CP violation disappears as two neutrinos become degenerate and/or as one of the angles, e. g. θ_{13} , is set to zero³⁷. Given the hierarchical nature of neutrino mass splittings, and the smallness of the mixing angle θ_{13} indicated by reactor experiments (see Sec. 3.3.1) it follows that probing CP violation effects in oscillation experiments will be a very demanding challenge. Therefore all such phases will be neglected in our discussion of solar and atmospheric neutrino oscillations.

In addition to the Majorana phases, the theoretically expected structure of leptonic weak interactions is substantially more complex in theories where neutrino masses arise from the so-called “see saw” mechanism^{21–23}. This follows from the fact that such models contain $SU(2) \otimes U(1)$ singlet leptons, so that the full charged current (CC) mixing matrix is rectangular, and the corresponding neutral current (NC) is non-trivial³⁴. In other words, the weak CC and NC interactions of neutrinos becomes non-standard. This implies yet additional angles and phases, which may lead to lepton flavour violation, and leptonic CP violation *even in the limit where neutrino masses would vanish*³⁸. This has the important implication that such processes are unrestricted by the smallness of neutrino mass. Given the many possible variants of the see-saw schemes³⁹, one finds that in some of such models the iso-singlet leptons need not be super-heavy⁴⁰, their masses lying at the weak scale or so. This leads to sizeable rates for lepton flavour and leptonic CP violating processes, unrelated to the magnitude of neutrino masses³⁸.

Insofar as neutrino propagation is concerned, we note that in this class of models the *effective* CC neutrino mixing matrix is not unitary, with a non-trivial neutrino mixing even in the massless limit⁴¹. This brings in the possibility of resonant oscillations of massless neutrinos in matter, first noted in ref.[41]. Effectively, neutrino propagation in matter is non-standard, as discussed in Sec. 5. For the time being we neglect all these subtle features in the description of neutrino oscillations we give in Sec. 3.

It may also happen that some of the $SU(2) \otimes U(1)$ singlet leptons are forced, e. g. by a protecting symmetry, to remain light enough to participate in the oscillations as *sterile neutrinos*⁴². Indeed, while the simplest three-neutrino picture is consistent with all other oscillation searches, it fails to account for the LSND hint¹⁴. Inclusion of the latter requires, in the framework of the oscillation hypothesis, the existence of a fourth light sterile neutrino taking part in the oscillations⁴². The presence of sterile neutrinos in the oscillations adds another mass parameter, and also increases the number of mixing parameters to six, in addition to CP phases. A detailed parametrization was first given in ref.[34]. A simple factorization convenient for use in a global analysis of oscillation data is illustrated in Fig. 1.

We will adopt this generalized framework in the description of solar and atmospheric oscillations⁹ presented in Sec. 3.1 where we describe, in particular, the constraints implied by both solar and atmospheric data samples on the sterile admixture, η_s . On the other hand this parametrization will also be employed in the global analysis⁴⁴ of all current oscillation data presented in Sec. 3.5.

2.2 The Absolute Scale of Neutrino Mass

Neutrino oscillations are sensitive only to mass splittings, not to the absolute scale of neutrino mass. Probing the latter requires either direct kinematical tests, using tritium beta spectrometers⁴⁵, or observations of the Cosmic Microwave Background and large scale structure, sensitive to a sub-leading hot dark matter component⁴⁶. The present limits come from a long list of painstaking efforts to study neutrino mass effects in beta decays, which culminated with the Mainz and Troitsk results (see ref.[45] for the corresponding references). Given the smallness of the solar and atmospheric mass splittings, the resulting (conservative) bounds on the sum of all neutrino masses^{46, 47}

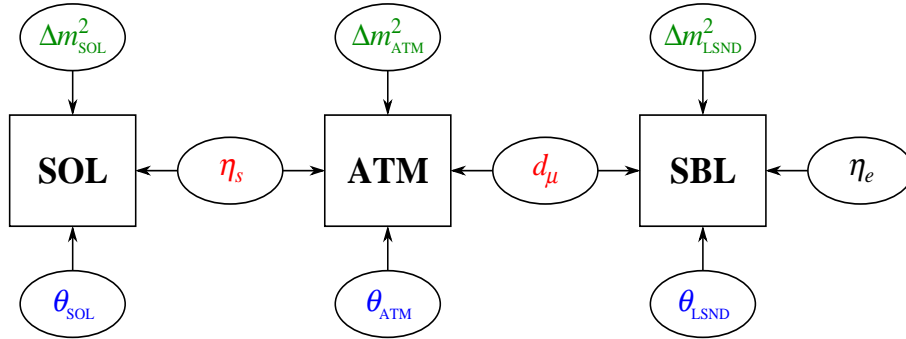


Fig. 1 Convenient separation of parameter dependence of the different data sets used in refs.[43] and [44].

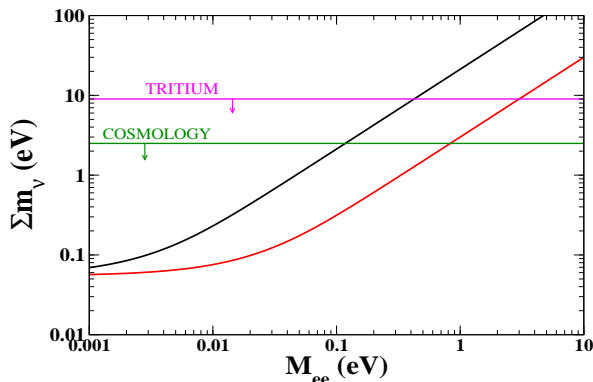


Fig. 2 $\beta\beta_{0\nu}$ and the scale of neutrino mass.

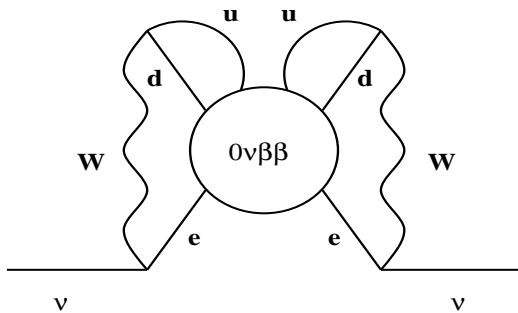


Fig. 3 The black-box $\beta\beta_{0\nu}$ argument⁴⁹.

are illustrated in the ordinate of Fig. 2.

To decide whether neutrinos are Dirac or Majorana particles requires the investigation of $\Delta L = 2$ (L denoting lepton-number) processes, of which $\beta\beta_{0\nu}$ decay provides the most classic example⁴⁸. Indeed, there is a *black-box theorem*⁴⁹ stating that, in a “natural” gauge theory, the observation of this process would signify the discovery that neutrinos are, as expected by theory³⁴, Majorana fermions. This connection is illustrated by Fig. 3.

The importance of this simple argument lies in its generality: it holds irrespective of how $\beta\beta_{0\nu}$ is engen-

dered. However, in order to quantify its implications, one needs to specify the particular model.

In the neutrino-exchange-induced mechanism, $\beta\beta_{0\nu}$ is characterized by an “effective” neutrino mass parameter M_{ee} whose value is sensitive to possible cancellations among individual neutrino amplitudes. These may arise either as a result of symmetries^{50, 51} or due to the Majorana-type *CP* phases³⁴. Nevertheless one can show that⁵², as illustrated in Fig. 2, there is a direct correlation between M_{ee} and the neutrino mass scales probed in tritium beta decays⁴⁷ and cosmology⁴⁶. It is therefore important to probe $\beta\beta_{0\nu}$ in a more sensitive experiment⁵³.

3 Neutrino Oscillations

Although the three-active neutrino oscillation scheme gives a good description of both solar and atmospheric data, we will follow the approach given in ref.[9] in which they are analysed in terms of mixed active-sterile neutrino oscillations. Such a generalized scheme has advantages that since it allows one to systematically combine solar and atmospheric data with the current short baseline neutrino oscillation data samples including the LSND evidence for oscillations⁴⁴, as shown later in this section. This is justified, since current reactor bounds on θ_{13} (Sec. 3.3.1) are stronger than solar and atmospheric bounds on the parameter η_s (with $0 \leq \eta_s \leq 1$, see Sec. 3.1) describing the fraction of sterile neutrinos taking part in the solar oscillations. By taking such simplified analysis with $\theta_{13} \rightarrow 0$, we completely decouple the solar and atmospheric oscillations from each other, and comply trivially with the strong constraints from reactor experiments. For a complementary earlier analysis with $\theta_{13} \neq 0$ effects, but no sterile neutrinos, see ref.[54]. As seen in Fig. 1, mixed

active-sterile neutrino oscillations are characterized by a total of six mixing angles³⁴.

3.1 Solar Neutrinos

The solar neutrino data include the solar neutrino rates of the chlorine experiment Homestake¹ ($2.56 \pm 0.16 \pm 0.16$ SNU), the most recent result of the gallium experiments³ SAGE ($70.8^{+5.3}_{-5.2} {}^{+3.7}_{-3.2}$ SNU) and GALLEX/GNO⁴ ($70.8 \pm 4.5 \pm 3.8$ SNU), as well as the 1496-days Super-Kamiokande data sample⁵. The latter are presented in the form of 44 bins (8 energy bins, 6 of which are further divided into 7 zenith angle bins). In addition to this, we have the latest results from SNO presented in ref.[6], for each day and night period). Therefore, in our statistical analysis there are $3 + 44 + 34 = 81$ observables.

The most popular explanation of solar neutrino experiments is provided by the neutrino oscillations hypothesis. For generality we follow the approach given in ref.[9] in which they are analysed in terms of mixed active-sterile neutrino oscillations, where the electron neutrino produced in the sun converts to ν_x (a combination of ν_μ and ν_τ) and a sterile neutrino ν_s : $\nu_e \rightarrow \sqrt{1 - \eta_s} \nu_x + \sqrt{\eta_s} \nu_s$.

In such a framework the solar neutrino data are fit with three parameters Δm_{SOL}^2 , θ_{SOL} and η_s . The parameter η_s with $0 \leq \eta_s \leq 1$ describes the fraction of sterile neutrinos taking part in the solar oscillations, so that when $\eta_s \rightarrow 0$ one recovers the conventional active oscillation case. The main motivation for adopting such generalized scenarios is the possibility of combining the solar and atmospheric data with short baseline oscillations⁴⁴. Four-neutrino mass schemes⁴² are the most natural candidates to accommodate solar and atmospheric mass-splittings with the hint from LSND¹⁴ indicating a large Δm^2 , see Sec. 3.3.

In Fig. 4 we display the regions of solar neutrino oscillation parameters for 3 d.o.f. with respect to the global minimum, for the standard case of active oscillations, $\eta_s = 0$, as well as for $\eta_s = 0.2$ and $\eta_s = 0.5$. The first thing to notice is the impact of the SNO NC, spectral, and day-night data in improving the determination of the oscillation parameters: the shaded regions after their inclusion are much smaller than the hollow regions delimited by the corresponding SNO_{CC}^{rate} confidence contours. Especially important is the full SNO_{CC,NC}^{SP,DN} information in closing the LMA-MSW region from above: Values of $\Delta m_{\text{SOL}}^2 > 10^{-3} \text{ eV}^2$ appear only at 3σ . Previous solar data on

their own could not close the LMA-MSW region, only the inclusion of reactor data¹⁸ probed the upper part of the LMA-MSW region⁵⁴. Furthermore, the complete SNO_{CC,NC}^{SP,DN} information is important for excluding *maximal* solar mixing in the LMA-MSW region. At 3σ with 1 d.o.f. one has

$$\text{LMA} - \text{MSW}: \quad 0.26 \leq \tan^2 \theta_{\text{SOL}} \leq 0.85, \\ 2.6 \times 10^{-5} \text{ eV}^2 \leq \Delta m_{\text{SOL}}^2 \leq 3.3 \times 10^{-4} \text{ eV}^2 \quad \dots (1)$$

showing that in the LMA-MSW region $\tan^2 \theta_{\text{SOL}}$ is significantly below maximal.

Note that in order to compare the allowed regions in Fig. 4 with others⁵⁵, one must note that our C.L. regions correspond to the 3 d.o.f. corresponding to $\tan^2 \theta_{\text{SOL}}$, Δm_{SOL}^2 and η_s . Therefore at a given C.L. our regions are larger than the usual regions for 2 d.o.f., because we also constrain the parameter η_s . Our global best fit point occurs for active oscillations with

$$\text{LMA} - \text{MSW}: \quad \tan^2 \theta_{\text{SOL}} = 0.46, \\ \Delta m_{\text{SOL}}^2 = 6.6 \times 10^{-5} \text{ eV}^2 \quad \dots (2)$$

A concise way to illustrate the above results is displayed in Fig. 5. We give the profiles of $\Delta \chi_{\text{SOL}}^2$ as a function of Δm_{SOL}^2 (left), $\tan^2 \theta_{\text{SOL}}$ (middle) as well as η_s (right), by minimizing with respect to the undisplayed oscillation parameters. In the left and middle panels the solid, dashed and dot-dashed lines correspond to $\eta_s = 0$, $\eta_s = 1$ and $\eta_s = 0.5$, respectively. The use of the full SNO_{CC,NC}^{SP,DN} sample has led to the relative worsening of all oscillation solutions with respect to the preferred active LMA-MSW solution. One sees also how the preferred status of the LMA-MSW solution survives in the presence of a small sterile admixture characterized by η_s . Increasing η_s leads to a deterioration of all oscillation solutions. Note that in the right panel we display the profile of $\Delta \chi_{\text{SOL}}^2$ as a function of $0 \leq \eta_s \leq 1$, irrespective of the detailed values of the solar neutrino oscillation parameters Δm_{SOL}^2 and θ_{SOL} . One can see that there is a crossing between the LMA-MSW and VAC solutions. This implies that the best pure-sterile description lies in the VAC regime. However, in the global analysis pure sterile oscillations with $\eta_s = 1$ are highly disfavoured. The χ^2 -difference between pure active and sterile is $\Delta \chi_{\text{s-a}}^2 = 32.2$ if one restricts to the LMA-MSW solution, or $\Delta \chi_{\text{s-a}}^2 = 23.3$ if one also allows for VAC. For

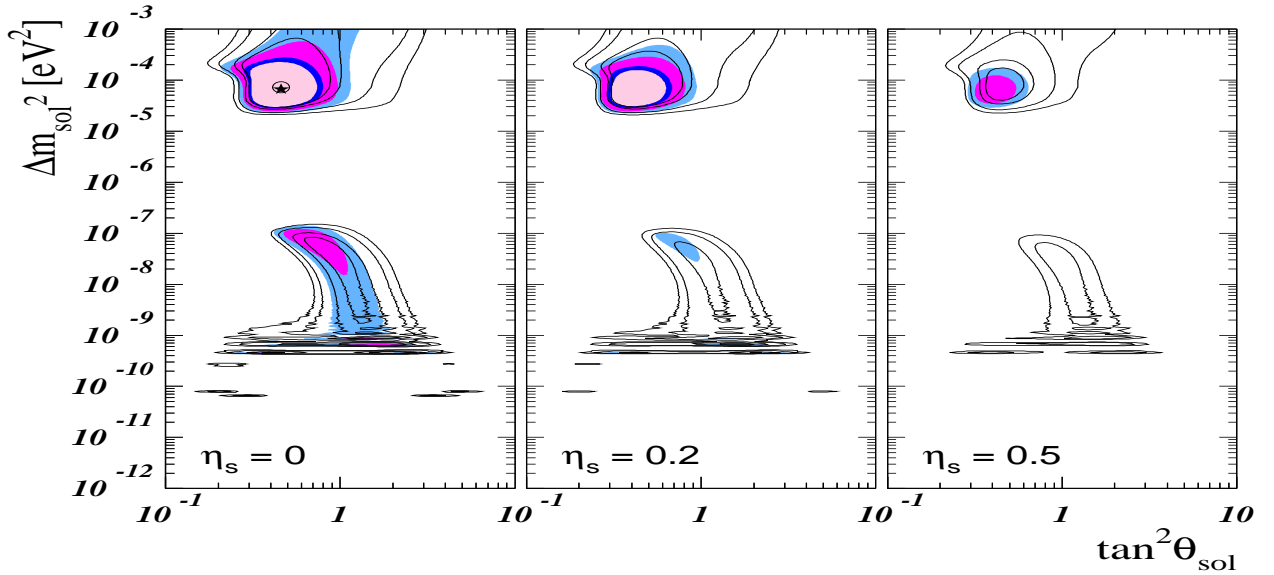


Fig. 4 Allowed $\tan^2 \theta_{\text{sol}}$ and Δm_{sol}^2 regions for $\eta_s = 0$ (active oscillations), $\eta_s = 0.2$ and $\eta_s = 0.5$. The lines and shaded regions correspond to the $\text{SNO}_{\text{CC}}^{\text{rate}}$ and $\text{SNO}_{\text{CC,NC}}^{\text{SP,DN}}$ analyses, respectively, as defined in ref.[9]. The 90%, 95%, 99% C.L. and 3σ contours are for 3 d.o.f..

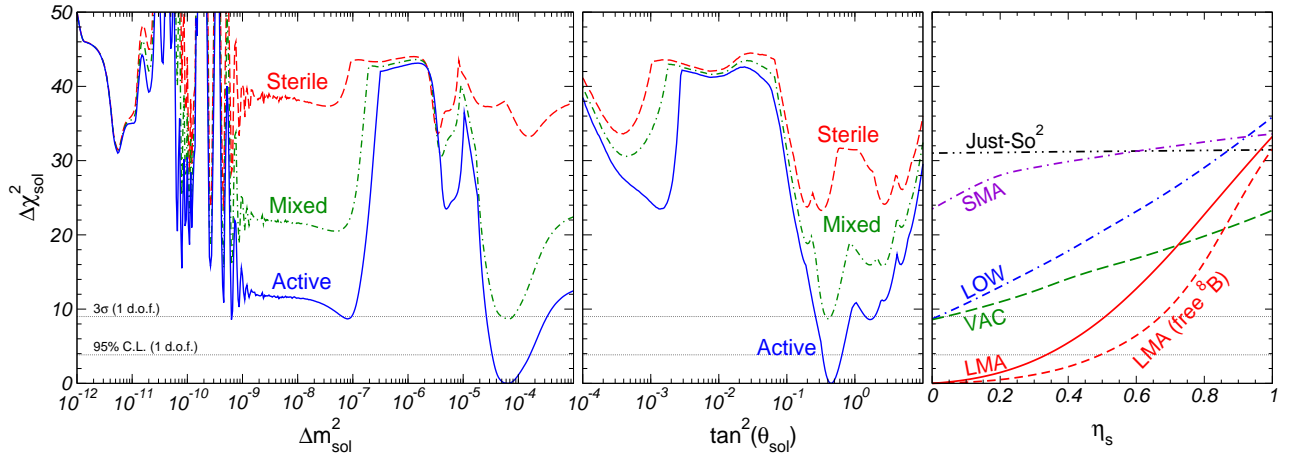


Fig. 5 $\Delta\chi_{\text{sol}}^2$ as a function of Δm_{sol}^2 , $\tan^2 \theta_{\text{sol}}$, and $0 \leq \eta_s \leq 1$ from global $\text{SNO}_{\text{CC,NC}}^{\text{SP,DN}}$ sample defined in ref.[9].

3 d.o.f. the $\Delta\chi_{s-a}^2 = 23.3$ implies that pure sterile oscillations are ruled out at 99.997% C.L. compared to the active case.

For the LMA-MSW solution one can also perform an analysis without fixing the boron flux to its SSM prediction, as seen in the right panel of Fig. 5. One can see that in this case the constraint on η_s is weaker than in the boron-fixed case, since a *small* sterile component can now be partially compensated by increasing the total boron flux coming from the Sun. From the figure one obtains the bounds

$$\text{solar data : } \eta_s \leq 0.44 \text{ (boron-fixed),}$$

$$\eta_s \leq 0.61 \text{ (boron-free) } \dots (3)$$

at 99% C.L. for 1 d.o.f.. A complete table of best fit values of Δm_{sol}^2 and θ_{sol} with the corresponding χ_{sol}^2 and GOF values for pure active, pure sterile, and mixed neutrino oscillations is given in ref.[9], both for the $\text{SNO}_{\text{CC}}^{\text{rate}}$ (48 – 2 d.o.f.) and the $\text{SNO}_{\text{CC,NC}}^{\text{SP,DN}}$ analysis (81 – 2 d.o.f.).

Comparing Different Solar Neutrino Analyses

Table I summarizes a compilation of the results of the solar neutrino analyses performed by the SNO and Super-K collaborations, as well as by different the-

oretical groups (see ref.[9] for the references). All groups find the best fit in the LMA-MSW region, although there are quantitative differences even for this preferred solution. As can be seen from the table, the GOF of the best-fit LMA-MSW solution, ranges from 53% to 97%.

Generally speaking, one expects the differences in the statistical treatment of the data to have little impact on the global best fit point, located in the LMA-MSW region. These differences typically become more visible as one compares absolute χ^2 values or departs from the best fit region towards more disfavoured solutions. Aware of this, ref.[9] took special care to details such as the dependence of the theoretical errors on the oscillation parameters entering the covariance matrix characterizing the Super-K and SNO electron recoil spectra. This ensures reliability of the results in the full $\tan^2 \theta_{\text{SOL}} - \Delta m_{\text{SOL}}^2$ plane.

The row labeled “d.o.f.” in the table gives the number of analysed data points minus the fitted parameters in each analysis. We also present the best fit values of $\tan^2 \theta_{\text{SOL}}$ and Δm_{SOL}^2 for active oscillations, the corresponding χ^2 -minima and GOF, as well as the $\Delta\chi^2$ with respect to the favoured active LMA-MSW solution. One can see from these numbers how various groups use different experimental input data, in particular the spectral and zenith angle information of Super-K and/or SNO. Despite differences in the analyzes there is relatively good agreement on the best fit active LMA-MSW parameters: the best fit values for $\tan^2 \theta_{\text{SOL}}$ are in the range 0.34 – 0.47 and for Δm_{SOL}^2 they lie in the range $(5.0 - 7.9) \times 10^{-5} \text{ eV}^2$. There is also good agreement on the allowed ranges of the oscillation parameters (not shown in the table). For example, the 3σ intervals given in Bahcall et al ($0.24 \leq \tan^2 \theta_{\text{SOL}} \leq 0.89$, $2.3 \times 10^{-5} \text{ eV}^2 \leq \Delta m_{\text{SOL}}^2 \leq 3.7 \times 10^{-4} \text{ eV}^2$) and Holanda-Smirnov ($\tan^2 \theta_{\text{SOL}} \leq 0.84$, $2.3 \times 10^{-5} \text{ eV}^2 \leq \Delta m_{\text{SOL}}^2 \leq 3.6 \times 10^{-4} \text{ eV}^2$) agree very well with those given in ref.[9]. There is remarkable agreement on the rejection of the LOW solution with respect to LMA-MSW with a $\Delta\chi_{\text{LOW,active}}^2 \approx 10$. The result for the vacuum solution in $^9 \Delta\chi_{\text{VAC,active}}^2 = 8.6$ is in good agreement with the values obtained by the Super-K collaboration, as well as Bahcall et al, de Holanda & Smirnov and Fogli et al, whereas Bandyopadhyay et al, Barger et al and Creminelli et al obtain higher values. For the SMA-MSW solution one finds $\Delta\chi_{\text{SMA,active}}^2 = 23.5$, in good agreement with the values obtained in Bahcall et

al, Creminelli et al and Fogli et al; while Bandyopadhyay et al and de Holanda & Smirnov, and especially Barger et al, obtain higher values. Typically the results of a given analysis away from the best fit LMA-MSW region serve as an indicator of its quality.

All in all, in view of the vast input data, of possible variations in the choice of the χ^2 function and the treatment of errors and their correlations, and of the complexity of the codes involved, it is encouraging that there is reasonable agreement amongst different analyzes, especially for the LMA-MSW solution. As shown in Sec. 3.4, LMA-MSW is now strongly preferred after the results of KamLAND described in Sec. 3.3.2. From this point of view it has now become somewhat academic to scrutinize further the origin of the differences found in the various analyzes. Nature has chosen the simplest solution.

3.2 Atmospheric Neutrinos

Here we summarize the analysis of atmospheric data given in a generalized oscillation scheme in which a light sterile neutrino takes part in the oscillations⁹. For simplicity the approximation $\Delta m_{\text{SOL}}^2 \ll \Delta m_{\text{ATM}}^2$ is used and the electron neutrino is taken as completely decoupled from atmospheric oscillations, by setting $\theta_{13} \rightarrow 0$ (for an analysis with $\theta_{13} \neq 0$ see ref.[54]). This way we comply with the strong constraints from reactor experiments in Sec 3.3.1. In contrast with the case of solar oscillations, the constraints on the ν_μ -content in atmospheric oscillations are not so stringent. Thus the description of atmospheric neutrino oscillations in this general framework requires *two new parameters* besides the standard two-neutrino oscillation parameters θ_{ATM} and Δm_{ATM}^2 . The parameters d_μ and d_s introduced in ref.[43] and illustrated in Fig. 1 are defined in such a way that $1 - d_\mu (1 - d_s)$ corresponds to the fraction of ν_μ (ν_s) participating in oscillations with Δm_{ATM}^2 . Hence, pure active atmospheric oscillations with Δm_{ATM}^2 are recovered when $d_\mu = 0$ and $d_s = 1$. In four-neutrino models there is a mass-scheme-dependent relationship between d_s and the solar parameter η_s . For details see ref.[43].

To get a feeling on for the physical meaning of these two parameters, note that for $d_\mu = 0$ the ν_μ oscillates with Δm_{ATM}^2 to a linear combination of ν_τ and ν_s given as $\nu_\mu \rightarrow \sqrt{d_s} \nu_\tau + \sqrt{1 - d_s} \nu_s$. For earlier pure active descriptions see, for example, refs.[57,58] and papers therein.

Table I

Comparison of different solar neutrino analyzes before KamLAND, from ref.[9]. See text.

	SNO Collaboration	Super-K Collaboration	Barger et al	Bandyopadhyay et al	Bahecall et al	Cremineili et al	Aliani et al	De Holanda & Smirnov	Fogli et al	Barranco et al, ref.[56]	Maltoni et al, ref.[9]
d.o.f.	75-3	46	75-3	49-4	80-3	49-2	41-4	81-3	81-3	81-2	81-2
best OSC-fit	active LMA-MSW solution										
$\tan^2 \theta_{\text{sol}}$	0.34	0.38	0.39	0.41	0.45	0.45	0.40	0.41	0.42	0.47	0.46
$\Delta m_{\text{sol}}^2 [10^{-5} \text{ eV}^2]$	5.0	6.9	5.6	6.1	5.8	7.9	5.4	6.1	5.8	5.6	6.6
χ_{LMA}^2	57.0	43.5	50.7	40.6	75.4	33.0	30.8	65.2	73.4	68.0	65.8
GOF	90%	58%	97%	66%	53%	94%	80%	85%	63%	81%	86%
$\Delta \chi_{\text{LOW}}^2$	10.7	79.0	79.2	10.0	79.6	78.1	–	12.4	10.0	–	78.7
$\Delta \chi_{\text{VAC}}^2$	–	10.0	25.6	15.5	10.1	14.?	–	79.7	77.8	–	78.6
$\Delta \chi_{\text{SMA}}^2$	–	15.4	57.3	30.4	25.6	23.?	–	34.5	23.5	–	23.5

The global best fit point occurs at

$$\sin^2 \theta_{\text{ATM}} = 0.49, \quad \Delta m_{\text{ATM}}^2 = 2.1 \times 10^{-3} \text{ eV}^2. \quad (4)$$

and has $d_s = 0.92$, $d_\mu = 0.04$. One sees that atmospheric data prefers a small sterile neutrino admixture. However, this is not statistically significant, since the pure active case ($d_s = 1, d_\mu = 0$) also gives an excellent fit: the difference in χ^2 with respect to the best fit point is only $\Delta \chi_{\text{act-best}}^2 = 3.3$. For the pure active best fit point one obtains,

$$\sin^2 \theta_{\text{ATM}} = 0.5, \quad \Delta m_{\text{ATM}}^2 = 2.5 \times 10^{-3} \text{ eV}^2 \dots (5)$$

with the 3σ ranges (1 d.o.f.)

$$0.3 \leq \sin^2 \theta_{\text{ATM}} \leq 0.7 \quad \dots (6)$$

$$1.2 \times 10^{-3} \text{ eV}^2 \leq \Delta m_{\text{ATM}}^2 \leq 4.8 \times 10^{-3} \text{ eV}^2 \dots (7)$$

The determination of the parameters θ_{ATM} and Δm_{ATM}^2 is summarized in Figs. 6 and 7. Note that Fig. 7 considers several cases: arbitrary d_s and d_μ , best-fit d_s and d_μ , and pure active and mixed active-sterile neutrino oscillations, as indicated.

At a given C.L. the χ_{ATM}^2 is cut at a $\Delta \chi^2$ determined by 4 d.o.f. to obtain 4-dimensional volumes in the parameter space of $(\theta_{\text{ATM}}, \Delta m_{\text{ATM}}^2, d_\mu, d_s)$. In the upper panels we show sections of these volumes at values of $d_s = 1$ and $d_\mu = 0$ corresponding to the pure active case (left) and the best fit point (right). Again one sees that moving from pure active to the best fit does not change the fit significantly. In the lower right panel both d_μ and d_s are projected away, whereas in the lower left panel $d_s = 0.5$ is fixed and one eliminates only d_μ . Comparing the regions resulting from 1489

days Super-K data (shaded regions) with the one from the 1289 days Super-K sample (hollow regions) we note that the new data leads to a slightly better determination of θ_{ATM} and Δm_{ATM}^2 . However, more importantly, from the lower left panel we see how the new data show a much stronger rejection against a sterile admixture: for $d_s = 0.5$ no allowed region appears at 3σ for 4 d.o.f..

The excellent quality of the neutrino oscillation description of the present atmospheric neutrino data can be better appreciated by displaying the zenith angle distribution of atmospheric neutrino events, given in Fig. 8. Clearly, active neutrino oscillations describe the data very well indeed. In contrast, the no-oscillations hypothesis can be visually spotted as being ruled out. On the other hand, conversions to sterile neutrinos lead to an excess of events for neutrinos crossing the core of the Earth, in all the data samples except sub-GeV.

3.3 Reactor and Accelerator Neutrino Data

3.3.1 Chooz and Palo Verde The Chooz experiment has been the first relatively long-baseline reactor neutrino experiment. As used in ref.[43], the measured $\bar{\nu}_e$ survival probability from these experiments are $P = 1.01 \pm 0.028 \pm 0.027$ for Chooz, and $P = 1.01 \pm 0.024 \pm 0.053$ for Palo Verde¹⁸. The non-observation of oscillations at these reactors provides an important restriction on Δm_{32}^2 and $\sin^2(2\theta_{13})$, as illustrated in Fig. 9. The curves represent the 90, 95 and 99% CL excluded region defined with 2 d.o.f. for comparison with the Chooz published results. For large Δm_{32}^2 this gives a stringent limit on $\sin^2(2\theta_{13})$, but not for low

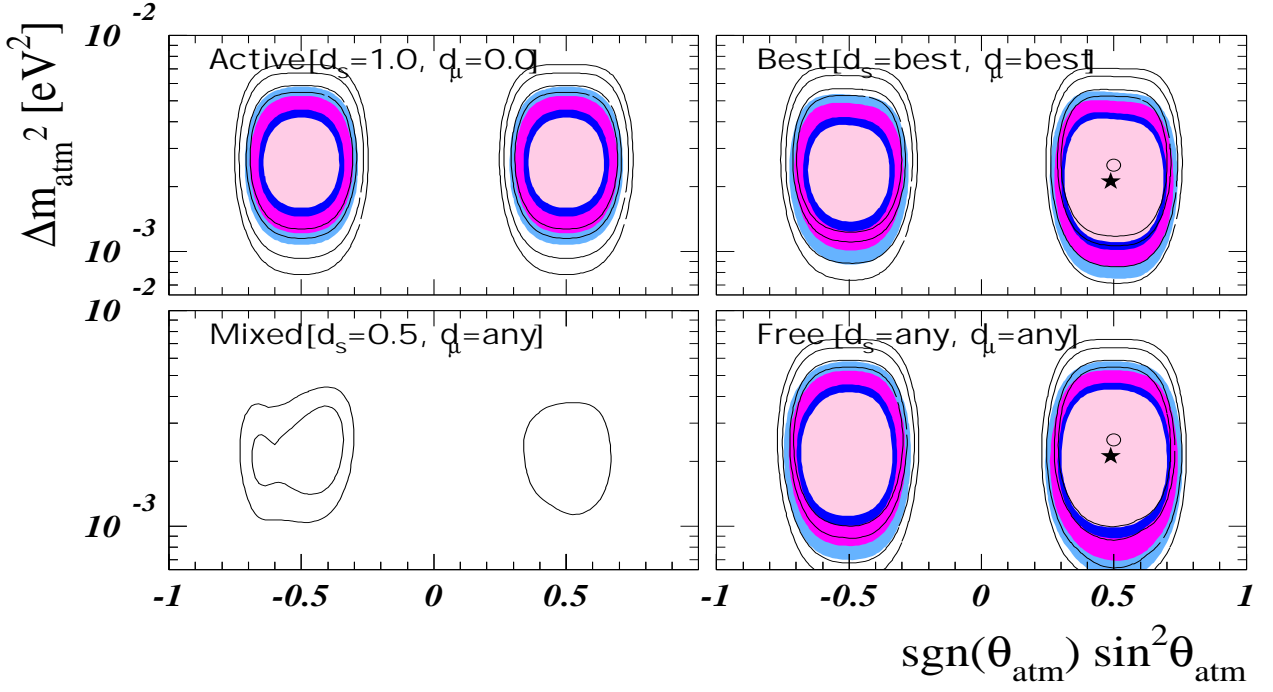


Fig. 6 Allowed regions of $\sin^2 \theta_{\text{ATM}}$ and Δm_{ATM}^2 at 90%, 95%, 99% and 3σ for 4 d.o.f. and different assumptions on the parameters d_s and d_μ , from⁹. The lines (shaded regions) correspond to 1289 (1489) days of Super-K data.

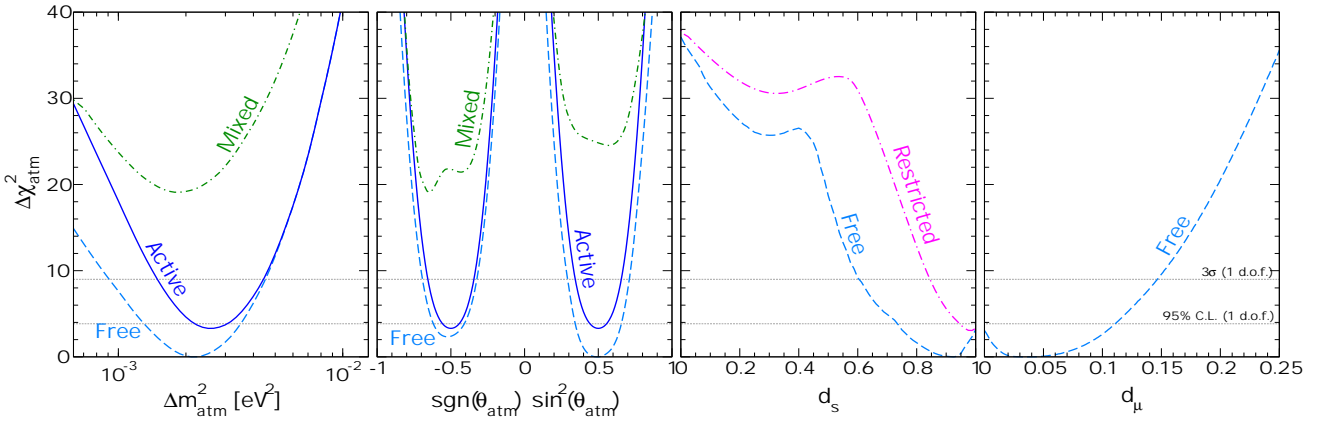


Fig. 7 $\Delta \chi_{\text{ATM}}^2$ as a function of Δm_{ATM}^2 , $\sin^2 \theta_{\text{ATM}}$, d_s and d_μ . In each panel the undisplayed parameters are integrated out. The “Mixed” and “Restricted” cases correspond to $d_s = 0.5$ and $d_\mu = 0$, respectively⁹.

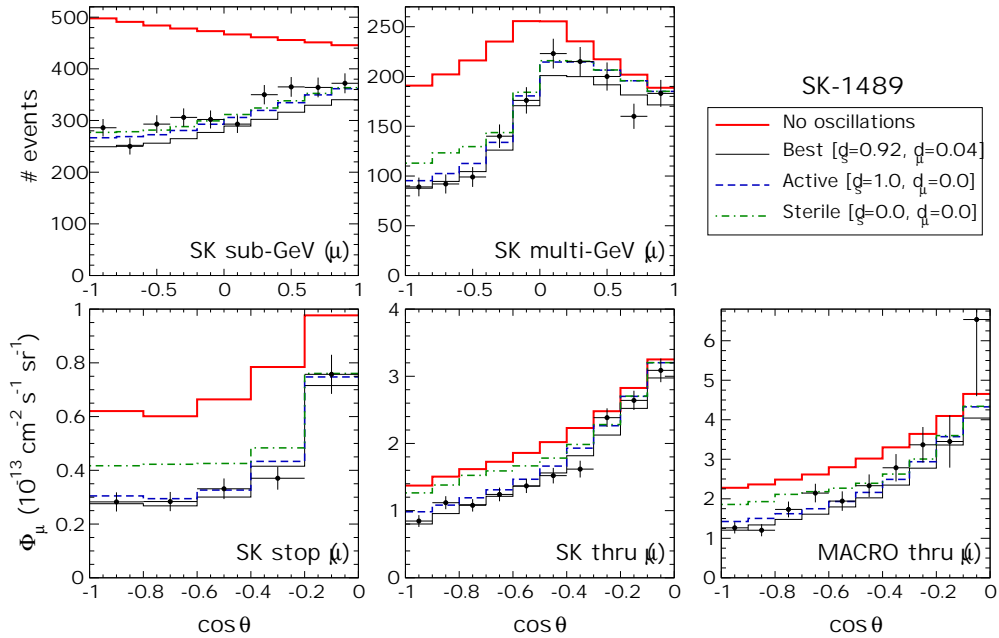


Fig. 8 Zenith angle dependence of the μ -like atmospheric neutrino data from ref.[9]. The predicted number of atmospheric neutrino events for best-fit, pure-active and pure-sterile oscillations and no oscillations are given, for comparison.

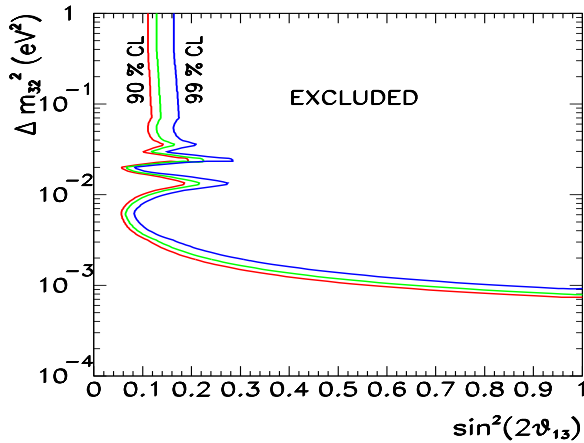


Fig. 9 Region in Δm_{32}^2 and $\sin^2(2\theta_{13})$ excluded by the Chooz reactor, from ref.[54].

Δm_{32}^2 values. Together with atmospheric data this implies that θ_{13} must be rather small. As will be seen below $\Delta m_{\text{ATM}}^2 \gg \Delta m_{\text{SOL}}^2$, i. e. one has a somewhat hierarchical structure of neutrino mass *splittings*.

3.3.2 KamLAND In the KamLAND reactor neutrino experiment the target for the $\bar{\nu}_e$ flux consists of a spherical transparent balloon filled with 1000 tons of non-doped liquid scintillator. The anti-neutrinos are detected via the inverse neutron β -decay

$$\bar{\nu}_e + p \rightarrow e^+ + n. \quad \dots (8)$$

The spectral data are given in 13 bins of prompt energy above 2.6 MeV in Fig. 5 of ref.[19].

There have been already several papers analysing the first results of the KamLAND experiment, here we follow ref.[59] The KamLAND data are simulated by calculating the expected number of events in each bin for given oscillation parameters as

$$N_i^{\text{th}}(\Delta m^2, \theta) = f \int dE_\nu \sigma(E_\nu) \times \sum_j \phi_j(E_\nu) P_j(E_\nu, \Delta m^2, \theta) \int dE_e R(E_e, E_e') \dots (9)$$

Here $R(E_e, E_e')$ is the energy resolution function and E_e, E_e' are the observed and the true positron energy, respectively, and an energy resolution of $7.5\%/\sqrt{E(\text{MeV})}$ is assumed¹⁹. The neutrino energy is related to the positron energy by $E_\nu = E_e' + \Delta$, where Δ is the neutron-proton mass difference. The integration interval over E_e is determined by the prompt energy interval in each bin. The neutrino spectrum $\phi(E_\nu)$ from nuclear reactors is well known, the phenomenological parameterization given in refs.[60,61] has been used. The average fuel composition for the nuclear reactors given in ref.[19] is adopted and possible effects due to time variations in the fuel composition have been neglected⁶¹. The sum over j in Eq. (9) runs over 16 nuclear plants, taking into account the different distances from the detector and the

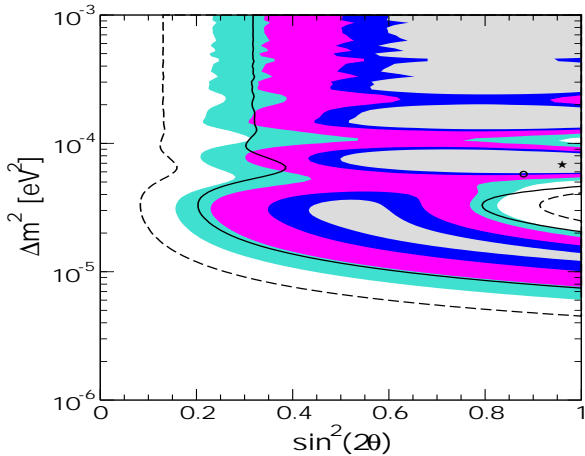


Fig. 10 Allowed regions at 90%, 95%, 99% and 99.73% C.L. (2 d.o.f.) from KamLAND spectral data. The solid (dashed) line is the 95% C.L. (3σ) region from the KamLAND rate alone. The star (dot) is the best fit point from the spectral (rate) analysis, from ref.[59].

power output of each reactor (see Table 3 of ref.[62]). The relevant detection cross section $\sigma(E_\nu)$ is given in ref.[63]. In the two-neutrino framework the disappearance probability for the neutrinos coming from the reactor j is given by

$$P_j(E_\nu, \Delta m^2, \theta) = 1 - \sin^2 2\theta \sin^2 \frac{\Delta m^2 L_j}{4E_\nu}. \dots (10)$$

The normalization factor f in Eq. (9) is determined in such a way that for the case of no oscillations the total number of events is 86.8, as expected from the Monte-Carlo simulation used in ref.[19].

For the statistical analysis one uses the χ^2 -function

$$\chi^2 = \sum_{i,j} (N_i^{\text{th}} - N_i^{\text{obs}}) S_{ij}^{-1} (N_j^{\text{th}} - N_j^{\text{obs}}). \dots (11)$$

The observed number of events N_j^{obs} in each bin can be read off from Fig. 5 of ref.[19]. In the covariance matrix one includes the statistical errors (obtained from the same figure) and the systematic error implied by the 6.42% uncertainty on the total number of events expected for no oscillations¹⁹.

In Fig.10 we show the allowed regions of the oscillation parameters obtained from our re-analysis of the KamLAND data. It is in good agreement with the analysis performed by the KamLAND collaboration, shown in Fig. 6 of ref.[19]. After this successful calibration we turn to a full global analysis combining also with the solar data sample in Sec. 3.4.

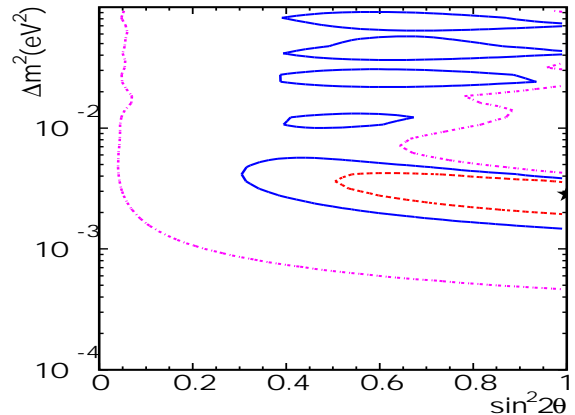


Fig. 11 Allowed regions of oscillation parameters from the K2K data of ref.[20]. Dashed, solid and dot-dashed lines are 68.4%, 90% and 99% C.L. contours, respectively. The best fit point is indicated by the star.

3.3.3 K2K Further evidence for the atmospheric neutrino anomaly has now come from the K2K experiment²⁰ using accelerator neutrinos in a long-baseline set-up. The collaboration sees a reduction of the ν_μ flux together with a distortion of the energy spectrum. They observe 56 beam neutrino events 250 km away from the neutrino production point, with an expectation of $80.1_{-5.4}^{+6.2}$. They also reconstruct the neutrino energy spectrum, which fits better the expected shape with neutrino oscillation than without. The probability that the observed flux at Super-K is a statistical fluctuation without neutrino oscillation is less than 1%.

The collaboration performs a two-neutrino oscillation analysis, with ν_μ disappearance, using the maximum-likelihood method, and including both the number of events and the energy spectrum shape. The results are given in Fig. 11 and agree nicely with what is inferred from the atmospheric analysis, Sec. 3.2.

3.3.4 LSND The Liquid Scintillating Neutrino Detector (LSND) is an experiment designed to search for neutrino oscillations in appearance channels. It is the only short baseline accelerator neutrino experiment claiming evidence for oscillations.

Here we compare the implications of two different analyses of the LSND data. The first uses the likelihood function obtained in the final LSND analysis¹⁴ from their global data with an energy range of $20 < E_e < 200$ MeV and no constraint on the likelihood ratio R_γ (see ref.[14] for details). This sample contains

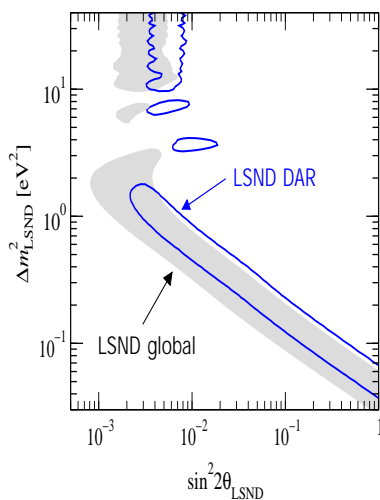


Fig. 12 Comparison of the 99% C.L. regions of the global LSND analysis¹⁴ (shaded region) and of the analysis in ref.[64] (solid line) using the decay-at-rest (DAR) sample. From ref.[44].

5697 events including decay-at-rest (DAR) $\bar{\nu}_\mu \rightarrow \bar{\nu}_e$, and decay-in-flight (DIF) $\nu_\mu \rightarrow \nu_e$ data. We refer to this analysis as *LSND global*. The second corresponds to the LSND analysis performed in ref.[64] based on 1032 events obtained from the energy range $20 < E_e < 60$ MeV and applying a cut of $R_\gamma > 10^{-5}$. These cuts eliminate most of the DIF events from the sample, leaving mainly the DAR data, which are more sensitive to the oscillation signal. We refer to this analysis as *LSND DAR*.

In both cases the likelihood function obtained in the analyses of the LSND collaboration was used and this was converted into a χ^2 according to $\chi^2 \propto -2 \ln \mathcal{L}$ (see ref.[43] for details). In Fig. 12 we compare the 99% C.L. regions obtained from the two LSND analyses. The LSND DAR data prefers somewhat larger mixing angles, which will lead to a stronger disagreement of the data in (3+1) oscillation schemes (see below). Furthermore, the differences in χ^2 between the best fit point and no oscillations for the two analyses are given by $\Delta\chi^2_{\text{no osc}} = 29$ (global) and $\Delta\chi^2_{\text{no osc}} = 47$ (DAR). This shows that the information leading to the positive oscillation signal seems to be more condensed in the DAR data. Note that the detailed information from the short baseline disappearance no-evidence experiments Bugey¹⁵ and CDHS¹⁶ has been fully taken into account. Concerning the constraints from KARMEN¹⁷, they are included by means of the KARMEN likelihood function.

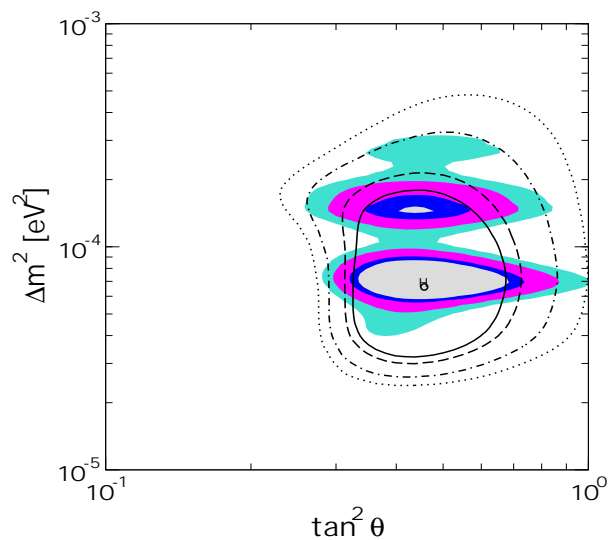


Fig. 13 Allowed regions at 90%, 95%, 99% and 99.73% C.L. (2 d.o.f.) from the combined analysis of solar, Chooz and KamLAND data. The hollow lines are the allowed regions from solar and Chooz data alone. The star (dot) is the best fit point from the combined (solar+Chooz only) analysis from ref.[59].

3.4 Neutrino Oscillations After KamLAND

There has been a rush of recent papers on the analysis of neutrino data after KamLAND in the framework of the neutrino oscillation hypothesis (assuming, of course, *CPT* invariance)^{59,65}. Here we discuss the results of the analysis presented in ref.[59], to which the reader is referred for the details. Figs. 13 and 14 summarize the results obtained in a combined fit of the full KamLAND data sample with the global sample of solar neutrino data (the same as used in ref.[9], as well as the Chooz result.

First of all, we have quantified the rejection of non-LMA solutions and found that it is now more robust. For example, for the LOW solution one has $\Delta\chi^2 = 26.9$, which for 2 d.o.f. (Δm^2_{SOL} and θ) lead to a relative probability of 1.4×10^{-6} . A similar result is also found for the VAC solution. Besides selecting out LMA-MSW as the unique solution of the solar neutrino problem we find, however, that the new reactor results have little impact on the location of the best fit point:

$$\tan^2 \theta = 0.46, \quad \Delta m^2_{\text{SOL}} = 6.9 \times 10^{-5} \text{ eV}^2 \dots (12)$$

In particular the solar neutrino mixing remains significantly non-maximal, a point which is not in conflict with the fact that KamLAND data alone pre-

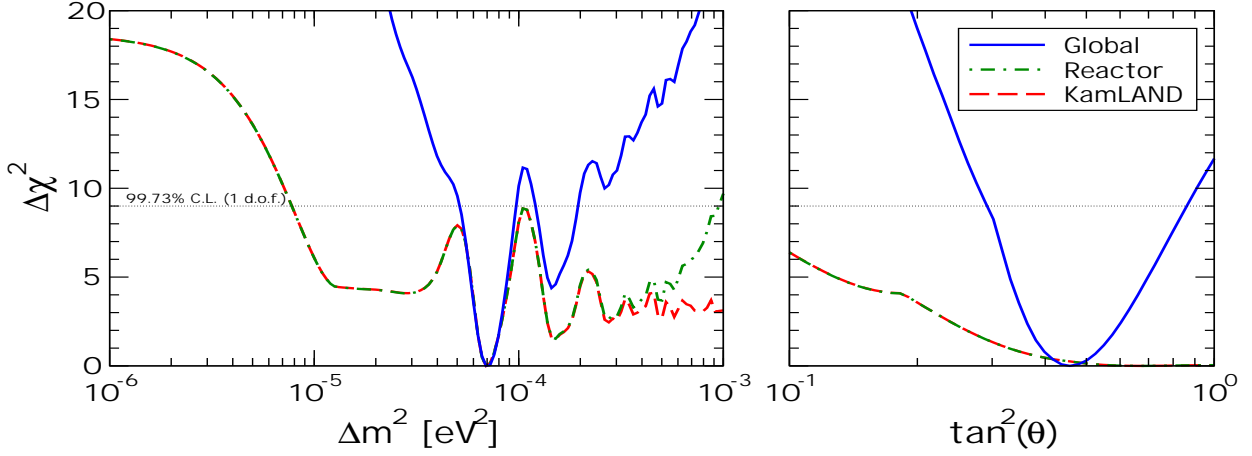


Fig. 14 $\Delta\chi^2$ versus Δm_{SOL}^2 and $\tan^2\theta$. The red dashed line refers to KamLAND alone. The green dot-dashed line corresponds to the full reactor data sample, including both KamLAND and Chooz. The blue solid line refers to the global analysis of the complete solar and reactor data, from ref.[59].

fer maximal mixing¹⁹, since this has no statistical significance⁵⁹. Indeed, one can see from the right panel in Fig. 14 that $\Delta\chi^2$ is rather flat with respect to the mixing angle for $\tan^2\theta \gtrsim 0.4$. This explains why the addition of the KamLAND data has no impact whatsoever on the determination of the solar neutrino oscillation mixing. The allowed 3σ region one finds for θ is:

$$0.29 \leq \tan^2\theta \leq 0.86, \quad \dots (13)$$

essentially the same as the pre-KamLAND range given in Eq. (1).

Note that the solar mixing angle is large, but significantly non-maximal, in contrast to the atmospheric mixing, Eq. (5). This important fact implies that models where the solar mixing is non-maximal³⁰ are strongly preferred over bi-maximal mixing models³¹.

Turning to the solar neutrino mass splittings, the new data do have a strong impact in narrowing down the allowed Δm_{SOL}^2 range. From the left panel of Fig. 14 one can see that the KamLAND data alone provides the bound $\Delta m_{\text{SOL}}^2 > 8 \times 10^{-6} \text{ eV}^2$, whereas the CHOOZ experiment gives $\Delta m_{\text{SOL}}^2 < 10^{-3} \text{ eV}^2$, both at 3σ . Hence global reactor neutrino data provide a robust allowed Δm_{SOL}^2 range, based only on terrestrial experiments. However, combining this information from reactors with the solar neutrino data leads to a significant reduction of the allowed range: As clearly visible in Fig. 13, the pre-KamLAND LMA-MSW region is now split into two sub-regions. At 3σ

(1 dof.) one obtains

$$5.1 \times 10^{-5} \text{ eV}^2 \leq \Delta m_{\text{SOL}}^2 \leq 9.7 \times 10^{-5} \text{ eV}^2 \dots (14)$$

$$1.2 \times 10^{-4} \text{ eV}^2 \leq \Delta m_{\text{SOL}}^2 \leq 1.9 \times 10^{-4} \text{ eV}^2 \dots (15)$$

This remaining ambiguity might be resolved when more KamLAND data have been collected^{61, 66, 67}.

3.5 Combining LSND Data with the Rest

A possible confirmation of the LSND anomaly would have remarkable implications. The most obvious would be the need for a sterile neutrino, which should be light enough to participate in the oscillations⁴². There are two classes of four-neutrino models, (3+1) and (2+2): in the first the sterile neutrino can decouple from both solar and atmospheric oscillations, while in the more symmetric (2+2) schemes, it cannot decouple from both sectors simultaneously⁴³. As a result (2+2) schemes are now more severely rejected by a global analysis.^b Fig. 15 shows the profiles of $\Delta\chi_{\text{SOL}}^2$, $\Delta\chi_{\text{ATM+SBL}}^2$ and $\bar{\chi}_{\text{global}}^2$ as a function of η_s in (2+2) oscillation schemes, as well as the values χ_{PC}^2 and χ_{PG}^2 relevant for the parameter consistency and parameter g.o.f. tests proposed in ref.[44]. The application of these tests to quantify the compatibility of LSND data with the remaining neutrino oscillation data in (3+1) schemes is illustrated in Fig.16. In the upper panel of Fig.16 we show the C.L. of the

^b Although KamLAND data are not included here, presently they have essentially no impact on the results presented in this section

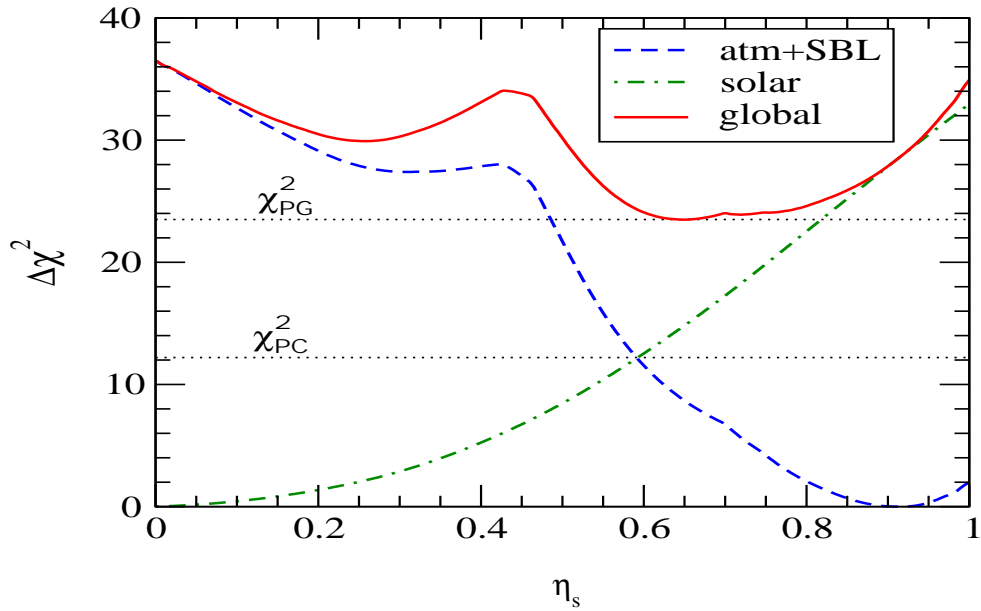


Fig. 15 Excluding joint (2+2) oscillation descriptions of current neutrino data including LSND, from ref.[44].

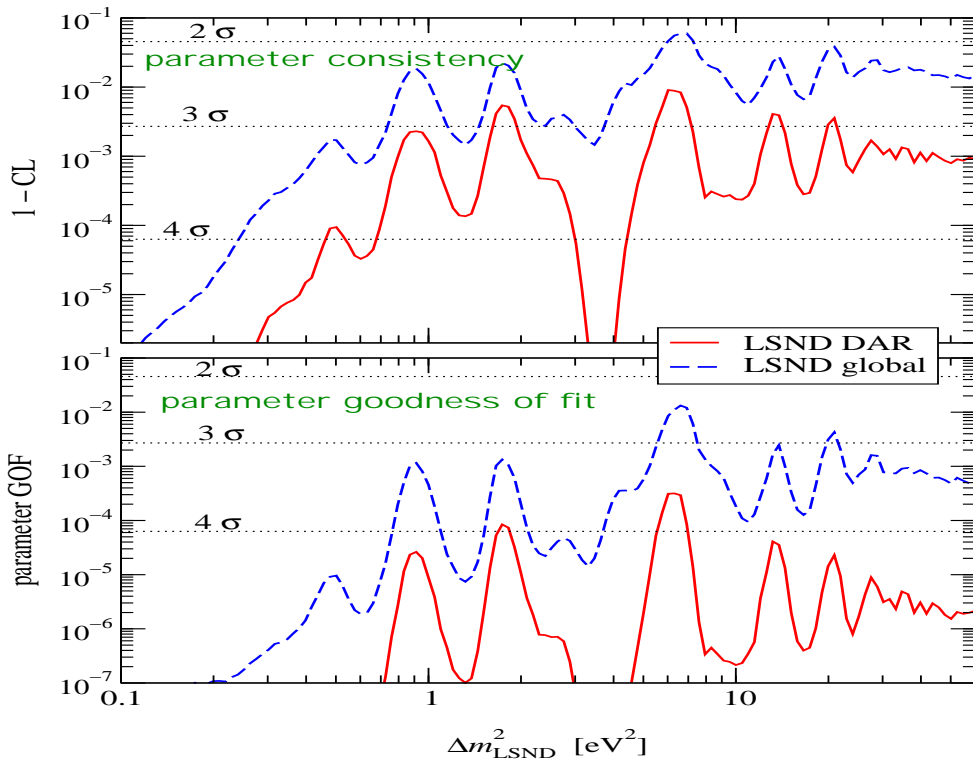


Fig. 16 Compatibility of LSND with solar+atmospheric+NEV data in (3+1) schemes, from ref.[44].

parameter consistency, whereas in the lower panel we show the parameter g.o.f. for fixed values of Δm_{LSND}^2 . The analysis is performed both for the global¹⁴ and for the DAR⁶⁴ LSND data samples. One sees that there is a slim chance to reconcile LSND data with the remaining data, provided Δm_{LSND}^2 is close to 6 eV^2 or so, but only at the expense of having a rather poor description.

In conclusion one finds that, though 4-neutrino models cannot be ruled out *per se*, the resulting global description of current neutrino oscillation data is extremely poor, even in the case of (3+1) schemes⁴⁴. We can only wait eagerly for news from the upcoming MiniBooNE experiment. Fortunately this experiment has begun collecting data in the last summer. If it turns out that MiniBooNE ultimately confirms the LSND claim we will face a real challenge.

4 Neutrino Mixing in Cosmology and Astrophysics

Neutrino flavour mixing usually has no observational consequences in Cosmology⁶⁸ because in the standard cosmological model all three neutrino flavours were produced in the early universe with identical spectra, and thus with the same energy and number densities. However, it could be that any of the neutrino chemical potentials was initially non-zero, or equivalently that a relic asymmetry between neutrinos and antineutrinos existed, which in turn increases the neutrino energy density and constitutes an extra radiation density. Only mild bounds on neutrino asymmetries exist from the analysis of CMBR anisotropies, while Primordial Big Bang Nucleosynthesis (BBN) places a more restrictive limit on the electron neutrino chemical potential, because the $\bar{\nu}_e$ participates directly in the beta processes that determine the primordial neutron-to-proton ratio.

As seen in Sec. 3.4, the KamLAND data have essentially fixed that neutrino oscillations explain the Solar Neutrino Problem with parameters in the LMA-MSW region. It was shown in ref.[69] that this result, combined with the evidence of oscillations of atmospheric neutrinos, implies that effective flavour equilibrium is established between all active neutrino species before BBN. Therefore the BBN constraints on the electron neutrino asymmetry apply to all flavours, which in turn implies that neutrino asymmetries do not significantly contribute to the extra rel-

ativistic degrees of freedom. Thus the number density of relic neutrinos is very close to its standard value, in such a way that future measurements of the absolute neutrino mass scale, for instance in the forthcoming tritium decay experiment KATRIN⁴⁵, will provide unambiguous information on the cosmic mass density in neutrinos, free of the uncertainty of neutrino chemical potentials.

If non-active light neutrino species exist, as suggested by the LSND data, then they are restricted also by BBN⁷⁰. However, this is less relevant now that the terrestrial data themselves disfavour the light sterile neutrino oscillation hypothesis.

Back to three-neutrinos, the effect of large solar neutrino mixing in astrophysics can be more substantial. First we note that the large solar mixing angle opens the possibility of probing the noisy character of the deep solar interior⁷¹, especially if an improved determination of Δm_{SOL}^2 is available from further KamLAND data.

Turning now to supernova neutrino spectra⁷², LMA-MSW neutrino conversions in a supernova environment induce a significant deformation of the energy spectra of neutrinos⁷³. Despite this fact, a global analysis of SN1987A and solar neutrino observations establishes the consistency of the LMA-MSW solution⁷⁴.

Nevertheless, the large solar mixing angle does have a strong impact on strategies for diagnosing collapse-driven supernovae through neutrino observations, opening new ways to probe supernova parameters. Indeed, fixing the LMA-MSW solution, one may in the future probe otherwise inaccessible features of supernova neutrino spectra such as the temperatures and luminosities of non-electron flavour neutrinos⁷⁵. This can be done simply by observing $\bar{\nu}_e$'s from galactic supernovae through the charged current reactions on protons, using massive water Cherenkov detectors. As an illustration we present in Fig. 17 different 3σ contours for Super-K and Hyper-K, calculated both for the case of LMA-MSW conversions and no-oscillations. Best fits are indicated by the stars. The plots result from a simulation which uses $\langle E_{\bar{\nu}_e}^0 \rangle = 15 \text{ MeV}$, $\tau^0 = 1.4$ and $E_b^0 = 3 \times 10^{53} \text{ erg}$ as input supernova parameters. Details can be found in ref.[75].

Recent simulations indicate, however, that although the value of τ^0 may be substantially lower than what has been optimistically assumed in ref.[75], the *fluxes* of different flavours of supernova neutrinos may

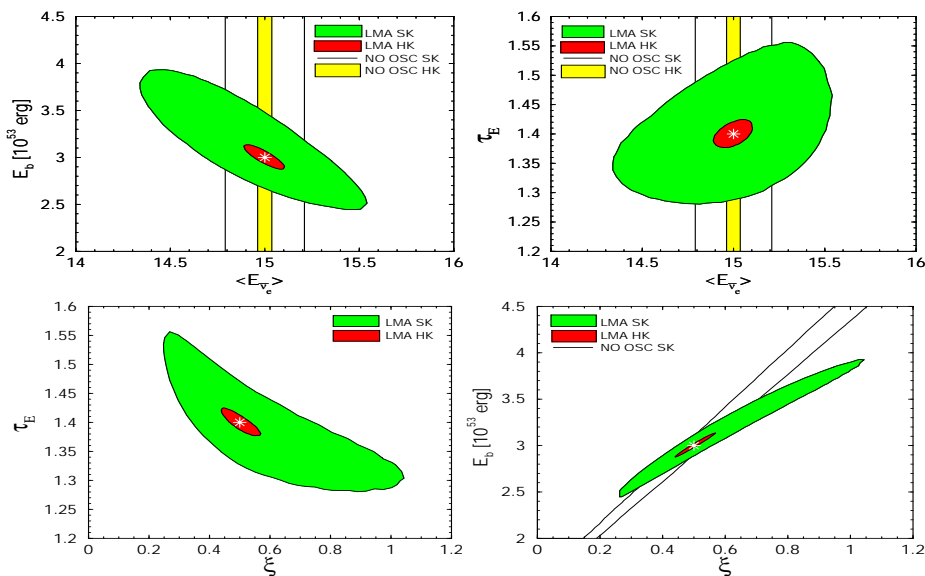


Fig. 17 Probing supernova spectra through LMA-MSW oscillations, from ref.[75]

differ⁷⁶, giving an additional handle on the diagnostic of supernovae through neutrino observations.

In addition to oscillations, other types of neutrino flavour conversions can affect the propagation of neutrinos in a variety of astrophysical environments, such as supernovae. For example, neutrino non-standard interactions, discussed in Sec. 5, could lead to resonant oscillations of massless neutrinos in matter⁴¹. These could lead to “deep-inside” conversions⁷⁷, rather distinct from those expected from conventional neutrino oscillations⁷⁸.

Another possibility is flavour conversion due to the decay of neutrinos, discussed in Sec. 7. If neutrino masses arise from the spontaneous violation of un-gauged lepton-number, they are accompanied by a physical Goldstone boson, the majoron²³. In the high-density supernova medium the effects of majoron-emitting neutrino decays are important even if they are suppressed in vacuum by small neutrino masses and/or small off-diagonal couplings. Such strong enhancement is due to matter effects, and implies that majoron-emitting decays have an important effect on the neutrino signal of supernovae⁷⁹. Majoron-neutrino coupling constants in the range $3 \times 10^{-7} \lesssim g \lesssim 2 \times 10^{-5}$ or $g \gtrsim 3 \times 10^{-4}$ are excluded by the observation of SN1987A, and could be probed with improved sensitivity from a future galactic supernova.

5 Non-Standard Neutrino Interactions

Non-standard neutrinos interactions (NSI) are a nat-

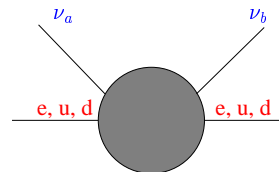


Fig. 18 Effective NSI operator.

ural feature in most neutrino mass models^{34,39}. They can be of two types: flavour-changing (FC) and non-universal (NU). The co-existence of neutrino masses and NSI in many models of neutrino mass means that neutrino flavour transformations may be induced by both and therefore ideally both should be taken into account when analysing neutrino data.

NSI may be schematically represented as effective dimension-6 terms of the type εG_F , as illustrated in Fig. 18, where ε specifies their sub-weak strength. Such interactions may arise from a nontrivial structure of CC and NC weak interactions characterized by a non-unitary lepton mixing matrix and a correspondingly non-trivial NC matrix³⁴. Such *gauge-induced* NSI may lead to flavour and *CP* violation, even with massless (degenerate) neutrinos⁴⁰. In radiative models where neutrino masses are “calculable”²⁵ and in supersymmetric models with broken R parity^{26,80} FC-NSI can also be *Yukawa-induced*, from the exchange of spinless bosons. In supersymmetric unified models, NSI may be calculable from renormalization effects⁸¹. We now describe the impact of non-standard neutrino

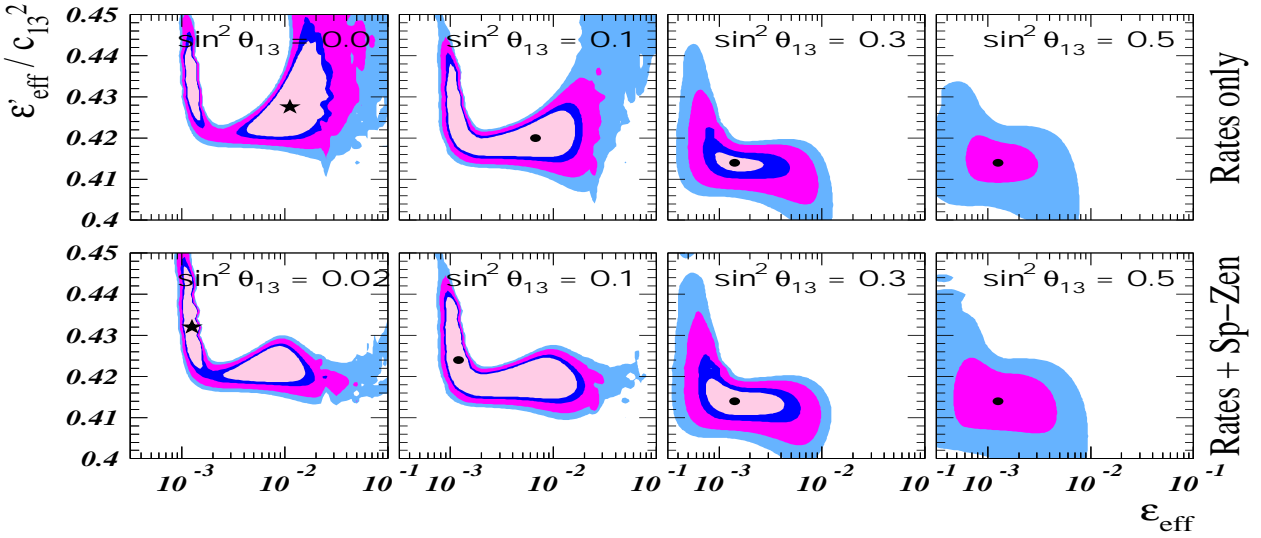


Fig. 19 Up-type quark NSI parameters needed to solve the solar neutrino anomaly, from the first of ref.[82].

interactions on solar and atmospheric neutrinos. Since the NSI strengths are highly model-dependent, we treat them as free phenomenological parameters.

5.1 Solar Neutrinos

At the moment one cannot yet pin down the exact profile of the ν_e survival probability over the whole spectrum and, as a result, the underlying mechanism of solar neutrino conversion remains unknown. Thus non-oscillation solutions, such as those based on non-standard neutrino matter interactions can be envisaged. As already mentioned, an important feature of the NSI-induced conversions⁴¹ is that the conversion probability is energy-independent. This implies that the solar neutrino energy spectrum is undistorted, as indeed preferred by the Super-K and SNO spectral data.

In the first paper in ref.[82] NSI provide an excellent description of present solar neutrino data. The allowed regions for the NSI mechanism of solar neutrino conversion are shown in Fig. 19. Although the required magnitude of NU interaction is somewhat large, it is not in conflict with current data^c. Moreover one sees that the amount of FC interaction indicated by the best fit is comfortably small.

Such a pure NSI description of solar data with massless and unmixed neutrinos is slightly better than that of the favoured LMA-MSW solution, and the NSI values indicated by the solar data analysis do not up-

set the successful oscillation description of the atmospheric data⁸². This establishes the overall consistency of a hybrid scheme in which only atmospheric data are explained in terms of neutrino oscillations. However, the recent first results of the KamLAND collaboration¹⁹ reject non-oscillation solutions, such as those based on NSI, at more than 3σ so that the NSI effect in solar neutrino propagation must be sub-leading. Accepting the LMA-MSW solution one may determine restrictions on NSI parameters and, therefore, on new aspects of neutrino mass models.

5.2 Atmospheric Neutrinos

Flavour-changing non-standard interactions (FC-NSI) in the $\nu_\mu - \nu_\tau$ channel have been shown to account for the zenith-angle-dependent deficit of atmospheric neutrinos observed in *contained* Super-K events⁸³. The solution works even in the absence of neutrino mass and mixing. However such pure NSI explanation fails to reconcile these with Super-K and MACRO *up-going muons*, due to the lack of energy dependence intrinsic to NSI conversions. The discrepancy is at the 99% C.L.⁵⁷. Thus, unlike the case of solar neutrinos, the oscillation interpretation of atmospheric data is robust, NSI being allowed only at a sub-leading level. Such robustness of the atmospheric $\nu_\mu \rightarrow \nu_\tau$ oscillation hypothesis can be used to provide the most stringent current limits on FC and NU neutrino interactions, as illustrated in Fig. 20. These lim-

^c Note that there are no stringent direct bounds on NSI involving neutrinos, only for the charged leptons. However, the latter do not directly apply to the neutrino case; hence the importance of the atmospheric data

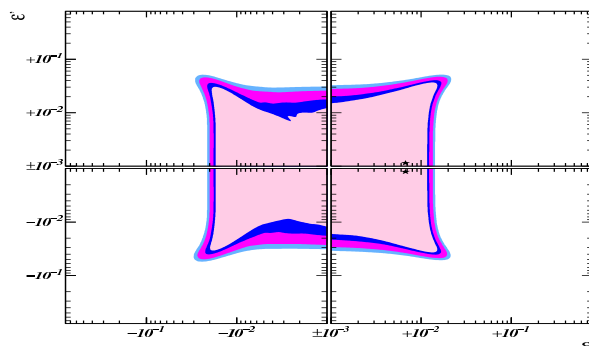


Fig. 20 Atmospheric bounds on neutrino NSI with down-type quarks⁵⁷.

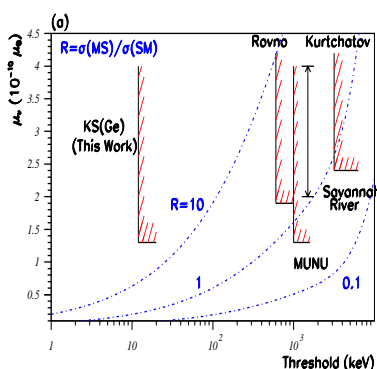


Fig. 21 Summary of the results in the searches of neutrino magnetic moments with reactor neutrinos, from ref.[86].

its are rather model-independent, as they are obtained from just neutrino-physics processes. As described in Sec. 9.5, future neutrino factories can probe non-standard neutrino interactions in this channel with better sensitivity.

6 Neutrino Magnetic Moments

6.1 Intrinsic Magnetic Moments

Non-zero neutrino masses can manifest themselves through non-standard neutrino electromagnetic properties. When the lepton sector in the Standard Model (SM) is minimally extended as in the quark sector, neutrinos get Dirac masses (m_ν) and their magnetic moments (MMs) are tiny⁸⁴,

$$\mu_\nu \simeq 3 \times 10^{-19} \mu_B \left(\frac{m_\nu}{\text{eV}} \right), \quad \dots (16)$$

where μ_B is the Bohr magneton. Laboratory experiments give 90% C.L. bounds on the neutrino MMs of $1.8 \times 10^{-10} \mu_B$ ⁸⁵ and $1.3 \times 10^{-10} \mu_B$ ^{86,87} for the electron neutrino. These are summarized in Fig. 21. For the muon neutrino⁸⁸ the bound is $6.8 \times 10^{-10} \mu_B$

and $3.9 \times 10^{-7} \mu_B$ for the tau neutrino⁸⁹ (see also ref.[47]). On the other hand, astrophysics and cosmology provide limits of the order of 10^{-11} to 10^{-12} Bohr magnetons⁹⁰. Improved sensitivity for the electron neutrino from reactor neutrino searches is expected, while a tritium $\bar{\nu}_e$ source experiment⁹¹ aims to reach the level $3 \times 10^{-12} \mu_B$.

It has for a long time been noticed, on quite general “naturalness” grounds, that Majorana neutrinos constitute the typical outcome of gauge theories³⁴. On the other hand, precisely such neutrinos also emerge in those employing the seesaw mechanism^{21–23}. If neutrinos are indeed Majorana particles the structure of their electromagnetic properties differs crucially from that of Dirac neutrinos⁹², being characterized by a 3×3 complex anti-symmetric matrix λ , the so-called Majorana transition moment (TM) matrix. It contains MMs as well as electric dipole moments of the neutrinos. The existence of any electromagnetic neutrino moment well above the expectation in Eq. (16) would signal the existence of physics beyond the SM. Thus neutrino electromagnetic properties are sensitive probes of new physics. Majorana TMs play an especially interesting role. As we will describe next, they can affect neutrino propagation in an important way and, to that extent, play an important in cosmology and astrophysics.

6.2 Spin Flavour Precession

Although LMA-MSW conversions are clearly favoured over other oscillation-type solutions, current solar neutrino data by themselves are not enough to single out the mechanism of neutrino conversion responsible for the suppression of the signal.

Magnetic-moment-induced neutrino conversions⁸⁴ in the convective zone of the Sun⁹³ have been long suggested as a potential solution of the solar neutrino problem. However, this would require too large a neutrino magnetic moment and also that neutrinos are Dirac particles, favoured neither by theory^{21–23} nor by astrophysics⁹⁴. As a result here we focus on the preferred case of Spin-flavour Precession (SFP)^{92,95}.

A global analysis of spin-flavour precession solutions to the solar neutrino problem, taking into account the impact of the full set of latest solar neutrino data, including the recent SNO-NC data as well as the 1496-day Super-Kamiokande data has been given in ref.[56]. These solutions depend in

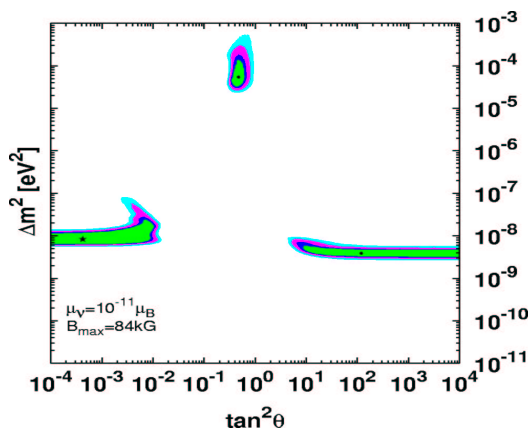


Fig. 22 Allowed Δm_{SOL}^2 and $\tan^2 \theta_{\text{SOL}}$ for RSFP, LMA-MSW and NRSFP solutions for the indicated values of μ, B , from ref.[56]

principle on the magnetic field profile. It is very convenient to adopt a self-consistent form for the static magnetic field profile^{96,97} motivated by magneto-hydrodynamics. With this one finds that, to a good approximation, the dependence of the neutrino SFP probabilities on the magnetic field gets reduced to an effective parameter μB_{\perp} characterizing the maximum magnetic field strength in the convective zone. This way one is left with just three parameters: $\Delta m_{\text{SOL}}^2 \equiv \Delta m^2$, the neutrino mixing angle $\theta_{\text{SOL}} \equiv \theta$ and the parameter μB_{\perp} . For $\mu = 10^{-11}$ Bohr magneton the lowest optimum B_{\perp} value is ~ 80 KGauss.

Fig. 22 shows the resulting parameter regions as given in ref.[56]. standard LMA-MSW solution, there are two SFP solutions, in the resonant (RSFP) and non-resonant (NRSFP) regimes⁹⁷, with LOW-quasi-vacuum or vacuum solutions absent at the 3 sigma level⁵⁶.

Note that in the presence of a neutrino transition magnetic moment of 10^{-11} Bohr magneton, a solar magnetic field of 80 KGauss eliminates all oscillation solutions other than LMA-MSW, irrespective of KamLAND results. On the other hand Fig. 23 shows the predicted solar neutrino survival probabilities for the “best” LMA-MSW solution, and for the “best” SFP solutions, from the latest solar data. Clearly the spectra in the high energy region are nearly undistorted in all three cases, in agreement with observations. As far as the solar neutrino data are concerned, one finds that the two SFP solutions give a slightly lower χ_{SOL}^2 than LMA-MSW, though all three solutions are statistically equivalent.

However, the recent first results announced by

the KamLAND collaboration¹⁹ imply that all non-oscillation solutions are strongly disfavoured. For the case of SFP solutions one finds a rejection at about 3σ , similar to that of non-LMA-MSW oscillation solutions before KamLAND.

7 Neutrino Decay

It is generally agreed that most probably neutrinos have non-zero masses and non-trivial mixings. This belief is based primarily on the evidence for neutrino mixings and oscillations from the solar and atmospheric neutrino data.

If neutrinos are massive they can decay. Current information on the absolute scale of neutrino mass from beta and double beta decay as well as cosmology suggests neutrino masses are at most of order of eV. Throughout the following discussion, we will stick to this assumption. In this case the only neutrino decay modes available within the simplest versions of the SM with massive neutrinos are radiative decays of the type $\nu' \rightarrow \nu + \gamma$ and so-called invisible decays such as the three-body decay $\nu' \rightarrow 3\nu$ ^{34,98} and two-body decays with majoron emission²³. The first one is “visible”, while the latter two are “invisible”.

The questions are (a) whether the lifetimes are short enough to be phenomenologically interesting and (b) what are the dominant decay modes. The answers to these are, unfortunately, rather model-dependent³⁹.

7.1 Radiative Decays

For eV neutrinos, the only radiative decay modes possible are $\nu_i \rightarrow \nu_j + \gamma$. They can occur at one-loop level in the SM. The decay rate is given by⁹⁹

$$\Gamma = \frac{9}{16} \frac{\alpha}{\pi} \frac{G_F^2}{128\pi^3} \frac{(\delta m_{ij}^2)^3}{m_i} \left| \sum_{\alpha} U_{i\alpha}^* U_{\alpha j} \left(\frac{m_{\alpha}^2}{m_W^2} \right) \right|^2 \quad \dots(17)$$

where $\delta m_{ij}^2 = m_i^2 - m_j^2$ and α runs over e, μ and τ . When $m_i \gg m_j, m_i \sim O(\text{eV})$ and for maximal mixing ($4U_{i\alpha}^* U_{\alpha j}^2 \sim O(1)$ and ($\alpha \cong \tau$) one obtains for Γ

$$\Gamma_{SM} \sim 10^{-45} \text{ sec}^{-1} \quad \dots(18)$$

which is far too small to be interesting. The decay mode $\nu_i \rightarrow \nu_j + \gamma$ comes from an effective coupling

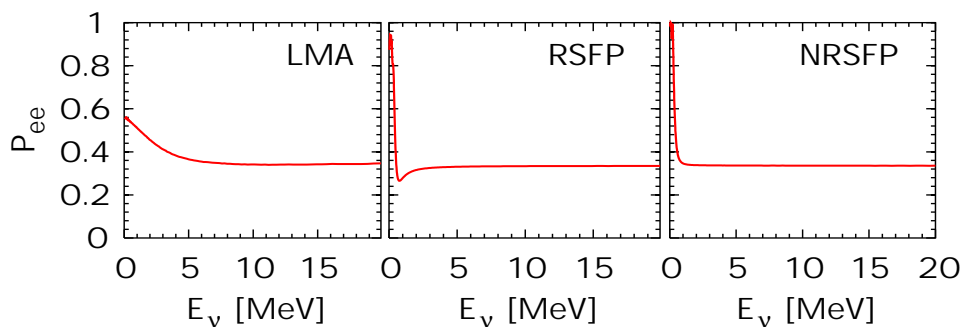


Fig. 23 Best LMA-MSW and SFP ν_e survival probabilities from⁵⁶

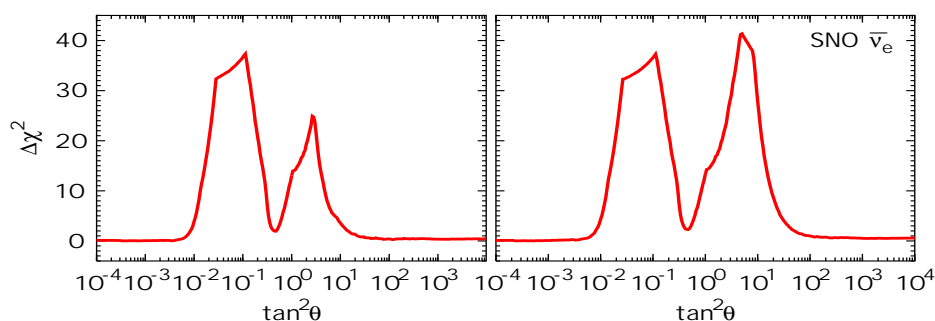


Fig. 24 $\Delta\chi_{\text{SOL}}^2$ versus $\tan^2 \theta_{\text{SOL}}$, for RSFP, LMA-MSW (central minima) and NRSFP solutions. Left and right panels refer to two different analyses described in ref.[56].

which can be written as:

$$\left(\frac{e}{m_i + m_j} \right) \bar{\psi}_j \sigma_{\mu\nu} (C + D\gamma_5) \psi_i F_{\mu\nu} \dots (19)$$

Let us define k_{ij} as

$$k_{ij} = \left(\frac{e}{m_i + m_j} \right) \sqrt{|C|^2 + |D|^2} \equiv k_0 \mu_B \dots (20)$$

where $\mu_B = e/2m_e$. Since the experimental bounds on μ_{ν_i} , the magnetic moments of neutrinos, come from reactions such as $\nu_e e \rightarrow e \nu$ which are not sensitive to the final state neutrinos, the bounds apply to both diagonal as well as transition magnetic moments and so can be used to limit k_0^i and the corresponding lifetimes. The current bounds are⁴⁷:

$$\begin{aligned} k_0^e &< 10^{-10}, & \dots (21) \\ k_0^\mu &< 7.4 \times 10^{-10}, \\ k_0^\tau &< 5.4 \times 10^{-7}. \end{aligned}$$

For $m_i \gg m_j$, the decay rate for $\nu_i \rightarrow \nu_j + \gamma$ is given by

$$\Gamma = \frac{\alpha}{2m_e^2} m_i^3 k_0^2 \dots (22)$$

This, in turn, gives indirect bounds on radiative decay lifetimes for $O(\text{eV})$ neutrinos of:

$$\begin{aligned} \tau_{\nu_e} &> 5 \times 10^{18} \text{ sec}, & \dots (23) \\ \tau_{\nu_\mu} &> 5 \times 10^{16} \text{ sec}, \\ \tau_{\nu_\tau} &> 2 \times 10^{11} \text{ sec}. \end{aligned}$$

We realize that it is the mass eigenstates which have well defined lifetimes. Converting these bounds to ones for flavour eigenstates would involve factors of mixing angles squared and with the large angles now indicated would change the above bounds by factors of 2 to 4.

There is one caveat in deducing these bounds. Namely, the form factors C and D are evaluated at $q^2 \sim O(\text{eV}^2)$ in the decay matrix elements whereas in the scattering from which the bounds are derived, they are evaluated at $q^2 \sim O(\text{MeV}^2)$. Thus, some extrapolation is necessary. It can be argued that, barring some bizarre behaviour, this is justified¹⁰⁰.

7.2 Invisible Neutrino Decays

7.2.1 Three-body Decays A decay mode with essentially invisible final states which does not involve any new particles is the three-body neutrino decay

mode, $\nu_i \rightarrow 3\nu$. In seesaw-type extensions of the standard electroweak theory these decays are mediated by the neutral-current⁹⁸, due to the admixture of isosinglet and isodoublets³⁴. As a result, in these theories there are nondiagonal couplings of the Z to the mass-eigenstate neutrinos, even at the tree level³⁴. The neutral current may be expressed in the following general form

$$P = K^\dagger K = \begin{pmatrix} K_L^\dagger K_L & K_L^\dagger K_H \\ K_H^\dagger K_L & K_H^\dagger K_H \end{pmatrix} \quad \dots(24)$$

where the matrix $P = P^2 = P^\dagger$ is directly determined in terms of the charged current lepton mixing matrix $K \equiv (K_L, K_H)$. The different entries in the P_{LL} sector of the P matrix determine the neutral current couplings of the light neutrinos that induce their decay. The deviation of P_{LL} from the identity matrix characterizes the departure from the GIM mechanism in the neutrino sector^{34, 98}. In seesaw models this is expected to be tiny, for neutrino masses in the eV range. Although it can be enhanced in variant seesaw type models^{40, 101} where the isosinglet heavy leptons are at the weak scale instead or possibly even lighter, this decay is still likely to be negligible.

Another way to induce this decay is through radiative corrections. Indeed, the $\nu_i \rightarrow 3\nu$ decay, like the radiative mode, can occur at one-loop level in SM. With a mass pattern $m_i \gg m_j$ the decay rate can be written as

$$\Gamma = \frac{\varepsilon^2 G_F^2 m_j^5}{192\pi^3}. \quad \dots(25)$$

In the SM at one-loop level, with the internal τ dominating, the value of ε^2 is given by¹⁰²

$$\varepsilon_{SM}^2 = \frac{3}{16} \left(\frac{\alpha}{\pi}\right)^2 \left(\frac{m_\tau}{m_W}\right)^4 \left\{ \ln\left(\frac{m_\tau^2}{m_W^2}\right) \right\}^2 \left(U_{\tau j} U_{\tau i}^*\right)^2 \quad \dots(26)$$

With maximal mixing $\varepsilon_{SM}^2 \approx 3 \times 10^{-12}$. Even if ε were as large as 1 with new physics contributions; it only gives a value for Γ of $5 \times 10^{-35} \text{ sec}^{-1}$. Hence, this decay mode will not yield decay rates large enough to be of interest. Although the current experimental bound on ε is quite poor: $\varepsilon < O(100)$, it is still strong enough to make this mode phenomenologically uninteresting, at least in vacuum.

7.2.2 Two-body Decays There is a wide variety of models where neutrinos get masses due to the spontaneous violation of global lepton number symmetry,

leading to a physical Nambu-Goldstone boson, called majoron. This leads to the most well-motivated candidate for invisible two-body neutrino decays^{23, 39}

$$\nu_{\alpha L} \rightarrow \nu_{\beta L} + J \quad \dots(27)$$

All couplings of the majoron vanish with the neutrino masses. The structure of the majoron coupling to mass-eigenstate neutrinos requires a careful diagonalization of the neutrino mass matrix⁹⁸. When one performs this, typically one finds that the majoron coupling matrix has a strong tendency of being diagonal. Such GIM-like effect is a generic feature of the simplest majoron schemes, first noted in ref.[98]. As a result, the off-diagonal couplings of the majoron to neutrino mass eigenstates relevant for the neutrino decays are strongly suppressed⁹⁸, so that neutrino decays become irrelevant^d.

However, majoron couplings are rather model-dependent³⁹, and it is possible to contrive models where they are sizeable enough to lead to lifetimes of phenomenological interest (the first example in ref.[104] is no longer phenomenologically viable, but it is possible to arrange many variants).

An alternative way to generate fast invisible two-body neutrino decays is in models with horizontal symmetries, spontaneously broken at a scale $\langle\sigma\rangle$, instead of lepton number¹⁰⁵. In this case there can be several Goldstone bosons (familons), characterized by $I=0, L=0, J=0$. Even if there is only one familon, its coupling is typically not subject to the kind of cancellation characteristic of majoron schemes, so that the new decay mode in eq. (27) has a decay rate

$$\Gamma = \frac{g_p^2 m_\alpha^3}{16\pi \langle\sigma\rangle^2} \quad \dots(28)$$

characterized by a dimensionless coupling g_p which is typically unsuppressed.

In the $SU(2)_L$ symmetry limit one has a similar coupling for the charged leptons, with corresponding decay modes $\ell_\alpha \rightarrow \ell_\beta + J$. Thus in this approximation the ν_α lifetime becomes related to the B.R. ($\ell_\alpha \rightarrow \ell_\beta + J$) through

$$\tau_{\nu_\alpha} = \frac{\tau_{\ell_\alpha}}{B.R.(\ell_\alpha \rightarrow \ell_\beta + J)} \left(\frac{m_{\nu_\alpha}}{m_{\ell_\alpha}}\right)^{-3} \quad \dots(29)$$

^d Similarly delicate is the issue of parametrizing the majoron couplings. If one is careful, one can show the full equivalence between polar (derivative couplings) and cartesian parametrizations¹⁰³.

The current bounds on μ and τ branching ratios^{47, 106}

$$\begin{aligned} B.R.(\mu \rightarrow eJ) &< 2 \times 10^{-6} \quad \dots(30) \\ B.R.(\tau \rightarrow \mu J) &< 7 \times 10^{-6} \end{aligned}$$

lead to

$$\begin{aligned} \tau_{\nu_\mu} &> 10^{24} \text{ sec} \quad \dots(31) \\ \tau_{\nu_\tau} &> 10^{20} \text{ sec.} \end{aligned}$$

These limits also hold for the case of an iso-doublet familon, $I = 1/2$, $L = 0$. In addition, one would need to fine tune in order to avoid mixing with the Standard Model Higgs.

However the $SU(2)_L$ symmetry is broken, so that the above simple argument is only a very crude approximation. The strongest direct bounds on neutrino-neutrino-Goldstone couplings is that which comes from a study of pion and kaon decays¹⁰⁷, but these bounds allow couplings strong enough that fast decays are certainly possible. A similar constraint⁵³ comes from $\beta\beta_{0\nu}$ ¹⁰⁸.

From now on we simply assume that fast invisible decays of neutrinos are possible, and ask ourselves whether such decay modes can be responsible for any of the observed neutrino anomalies.

We assume a component of ν_α , i.e., ν_2 , to be the only unstable state, with a rest-frame lifetime τ_0 , and we assume two-flavour mixing, for simplicity:

$$\nu_\alpha = \cos \theta \nu_2 + \sin \theta \nu_1 \quad \dots(32)$$

with $m_2 > m_1$. From Eq. (2) with an unstable ν_2 , the ν_α survival probability is

$$\begin{aligned} P_{\alpha\alpha} &= \sin^4 \theta + \cos^4 \theta \exp(-\alpha L/E) \quad \dots(33) \\ &+ 2 \sin^2 \theta \cos^2 \theta \exp(-\alpha L/2E) \cos(\delta m^2 L/2E), \end{aligned}$$

where $\delta m^2 = m_2^2 - m_1^2$ and $\alpha = m_2/\tau_0$. Since we are attempting to explain neutrino data without oscillations there are two appropriate limits of interest. One is when the δm^2 is so large that the cosine term averages to 0. Then the survival probability becomes

$$P_{\mu\mu} = \sin^4 \theta + \cos^4 \theta \exp(-\alpha L/E) \quad \dots(34)$$

Let this be called decay scenario A. The other possibility is when δm^2 is so small that the cosine term is 1, leading to a survival probability of

$$P_{\mu\mu} = (\sin^2 \theta + \cos^2 \theta \exp(-\alpha L/2E))^2 \dots(35)$$

corresponding to decay scenario B.

The possibility of solar neutrinos decaying to explain the discrepancy is a very old suggestion¹⁰⁹. The most recent analysis of the current solar neutrino data finds that no good fit can be found¹¹⁰; the conclusion is valid for both the decay scenarios A as well as B.

For atmospheric neutrinos, it was found that for the decay scenario A, it was not possible to obtain a good fit for all energies. Turning to decay scenario B, a reasonable fit was obtained for all the atmospheric data, with a minimum $\chi^2 = 33.7$ (32 d.o.f.) for the choice of parameters

$$\tau_\nu/m_\nu = 63 \text{ km/GeV}, \quad \cos^2 \theta = 0.30 \quad \dots(36)$$

The fit is of comparable quality as the for one with oscillations¹¹¹.

The reason for the similarity of the results obtained in the two models can be understood from the fact that the survival probability $P(\nu_\mu \rightarrow \nu_\mu)$ of muon neutrinos as a function of L/E_ν for the two models using the best fit parameters is very similar. In the case of the neutrino decay model the probability $P(\nu_\mu \rightarrow \nu_\mu)$ monotonically decreases from unity to an asymptotic value $\sin^4 \theta \simeq 0.49$. In the case of oscillations the probability has a sinusoidal behaviour in L/E_ν . The two functional forms seem very different; however, taking into account the resolution in L/E_ν , the two forms are hardly distinguishable. In fact, in the large L/E_ν region, the oscillations are averaged out and the survival probability there can be well-approximated with 0.5 (for maximal mixing). In the region of small L/E_ν both probabilities approach unity. In the region L/E_ν around 400 km/GeV, where the probability for the neutrino oscillation model has the first minimum, the two curves are most easily distinguishable, at least in principle. It is entirely possible that the Super-K data and new analysis of this most recent decay model can eventually rule this out. K2K and eventually MINOS can also test this hypothesis¹¹².

Assuming that the neutrino oscillations provide the most likely explanation for the bulk of both atmospheric and solar neutrino observations; is it possible to place limits on the neutrino lifetimes? It is obvious that solar neutrino data will provide the strongest bounds currently possible. It has been argued convincingly by Beacom and Bell recently that under the most general assumptions the bound on the lifetime of ν_e (or the dominant mass eigenstate components thereof) is $\tau > 10^{-4}$ sec for mass in the eV range¹¹³.

The strongest bounds can be obtained in the future from observation of MeV neutrinos from a Galactic supernova ($\tau \sim 10^5$ sec) or high energy neutrinos from AGNs ($\tau \sim 10^3$ sec)¹¹⁴.

8 CPT and Lorentz Violation

8.1 CPT Violation in Neutrino Oscillations

Consequences of CP , T and CPT violation for neutrino oscillations have been written down before^{35, 115}. We summarise them briefly for the $\nu_\alpha \rightarrow \nu_\beta$ flavour oscillation probabilities $P_{\alpha\beta}$ at a distance L from the source. If

$$P_{\alpha\beta}(L) \neq P_{\bar{\alpha}\bar{\beta}}(L), \quad \beta \neq \alpha, \quad \dots(37)$$

then CP is not conserved. If

$$P_{\alpha\beta}(L) \neq P_{\beta\alpha}(L), \quad \beta \neq \alpha, \quad \dots(38)$$

then T -invariance is violated. If

$$P_{\alpha\beta}(L) \neq P_{\bar{\beta}\bar{\alpha}}(L), \quad \beta \neq \alpha, \quad \dots(39)$$

or

$$P_{\alpha\alpha}(L) \neq P_{\bar{\alpha}\bar{\alpha}}(L), \quad \dots(40)$$

then CPT is violated. When neutrinos propagate in matter, matter effects give rise to apparent CP and CPT violation even if the mass matrix is CP conserving. The CPT violating terms can be Lorentz-invariance violating (LV) or Lorentz invariant. The Lorentz-invariance violating, CPT violating case has been discussed by Colladay and Kostelecky¹¹⁶ and by Coleman and Glashow¹¹⁷.

The effective LV CPT violating interaction for neutrinos is of the form

$$\bar{\nu}_L^\alpha b_\mu^{\alpha\beta} \gamma_\mu \nu_L^\beta, \quad \dots(41)$$

where α and β are flavour indices. If rotational invariance is assumed in the ‘‘preferred’’ frame, in which the cosmic microwave background radiation is isotropic, then the neutrino energies are eigenvalues of

$$m^2/2p + b_0, \quad \dots(42)$$

where b_0 is a hermitian matrix, hereafter labeled b . In the two-flavour case the neutrino phases may be chosen such that b is real, in which case the interaction

in Eq. (41) is CPT odd. The survival probabilities for flavours α and $\bar{\alpha}$ produced at $t = 0$ are given by¹¹⁸

$$P_{\alpha\alpha}(L) = 1 - \sin^2 2\Theta \sin^2(\Delta L/4), \quad \dots(43)$$

and

$$P_{\bar{\alpha}\bar{\alpha}}(L) = 1 - \sin^2 2\bar{\Theta} \sin^2(\bar{\Delta} L/4), \quad \dots(44)$$

where

$$\Delta \sin 2\Theta = \left| (\delta m^2/E) \sin 2\theta_m + 2\delta b e^{i\eta} \sin 2\theta_b \right|, \quad \dots(45)$$

$$\Delta \cos 2\Theta = (\delta m^2/E) \cos 2\theta_m + 2\delta b \cos 2\theta_b. \quad \dots(46)$$

$\bar{\Delta}$ and $\bar{\Theta}$ are defined by similar equations with $\delta b \rightarrow -\delta b$. Here θ_m and θ_b define the rotation angles that diagonalize m^2 and b , respectively, $\delta m^2 = m_2^2 - m_1^2$ and $\delta b = b_2 - b_1$, where m_i^2 and b_i are the respective eigenvalues. We use the convention that $\cos 2\theta_m$ and $\cos 2\theta_b$ are positive and that δm^2 and δb can have either sign. The phase η in Eq. (45) is the difference of the phases in the unitary matrices that diagonalize δm^2 and δb ; only one of these two phases can be absorbed by a redefinition of the neutrino states. Observable CPT -violation in the two-flavour case is a consequence of the interference of the δm^2 terms (which are CPT -even) and the LV terms in Eq. (41) (which are CPT -odd); if $\delta m^2 = 0$ or $\delta b = 0$, then there is no observable CPT -violating effect in neutrino oscillations. If $\delta m^2/E \gg 2\delta b$ then $\Theta \simeq \theta_m$ and $\Delta \simeq \delta m^2/E$, whereas if $\delta m^2/E \ll 2\delta b$ then $\Theta \simeq \theta_b$ and $\Delta \simeq 2\delta b$. Hence the effective mixing angle and oscillation wavelength can vary dramatically with E for appropriate values of δb . We note that a CPT -odd resonance for neutrinos ($\sin^2 2\Theta = 1$) occurs whenever $\cos 2\Theta = 0$ or

$$(\delta m^2/E) \cos 2\theta_m + 2\delta b \cos 2\theta_b = 0; \quad \dots(47)$$

similar to the resonance due to matter effects^{10, 118}. The condition for antineutrinos is the same except δb is replaced by $-\delta b$. The resonance occurs for neutrinos if δm^2 and δb have the opposite sign, and for antineutrinos if they have the same sign. A resonance can occur even when θ_m and θ_b are both small, and for all values of η ; if $\theta_m = \theta_b$, a resonance can occur only if $\eta \neq 0$. If one of ν_α or ν_β is ν_e , then matter effects have to be included.

If $\eta = 0$, then

$$\Theta = \theta, \quad \dots(48)$$

$$\Delta = (\delta m^2/E) + 2\delta b. \quad \dots(49)$$

In this case a resonance is not possible. The oscillation probabilities become

$$P_{\alpha\alpha}(L) = 1 - \sin^2 2\theta \sin^2 \left\{ \left(\frac{\delta m^2}{4E} + \frac{\delta b}{2} \right) L \right\}, \quad \dots (50)$$

$$P_{\bar{\alpha}\bar{\alpha}}(L) = 1 - \sin^2 2\theta \sin^2 \left\{ \left(\frac{\delta m^2}{4E} - \frac{\delta b}{2} \right) L \right\}. \quad \dots (51)$$

For fixed E , the δb terms act as a phase shift in the oscillation argument; for fixed L , the δb terms act as a modification of the oscillation wavelength. An approximate direct limit on δb when $\alpha = \mu$ can be obtained by noting that in atmospheric neutrino data the flux of downward going ν_μ is not depleted, whereas that of upward going ν_μ is depleted¹². Hence, the oscillation arguments in Eqs. (50) and (51) cannot have fully developed for downward neutrinos. Taking $|\delta b L/2| < \pi/2$ with $L \sim 20$ km for downward events leads to the upper bound $|\delta b| < 3 \times 10^{-20}$ GeV; the K2K results can improve this by an order of magnitude; upward going events could in principle test $|\delta b|$ as low as 5×10^{-23} GeV. Since the CPT -odd oscillation argument depends on L and the ordinary oscillation argument on L/E , improved direct limits could be obtained by a dedicated study of the energy and zenith angle dependence of the atmospheric neutrino data.

The difference between $P_{\alpha\alpha}$ and $P_{\bar{\alpha}\bar{\alpha}}$

$$P_{\alpha\alpha}(L) - P_{\bar{\alpha}\bar{\alpha}}(L) = -2 \sin^2 2\theta \sin \left(\frac{\delta m^2 L}{2E} \right) \sin(\delta b L), \dots (52)$$

can be used to test for CPT -violation. In a neutrino factory, the ratio of $\bar{\nu}_\mu \rightarrow \bar{\nu}_\mu$ to $\nu_\mu \rightarrow \nu_\mu$ events will differ from the Standard Model (or any local quantum field theory model) value if CPT is violated. A 10kT detector, with 10^{19} stored muons, can probe δb to a level of $3 \cdot 10^{-23}$ GeV¹¹⁹. Combining KamLAND and solar neutrino data would probe δb to similar levels. Lorentz invariant CPT violation can arise if e.g. δm_{ij}^2 and θ_{ij} are different for neutrinos and antineutrinos. Constraints on such differences are rather weak¹¹⁸. Taking advantage of this, a very intriguing proposal has been made by several authors¹²⁰. It was proposed that in the ν sector, the δm^2 and mixing are ‘‘conventional’’ and nearly bimaximal; namely δm_{23}^2 and δm_{21}^2 lie in the atmospheric range determined in Sec. 3.2 and in the LMA-MSW region determined in

Secs. 3.1, respectively. In contrast, in the $\bar{\nu}$ sector $\delta m_{23}^2 \sim 0(eV^2)$, δm_{21}^2 lies in the atmospheric range and the mixing is large in the 1-2 sector but small (of order LSND) in 2-3 sector. Then the $\bar{\nu}_\mu - \bar{\nu}_e$ conversion in LSND¹⁴ is accounted for, and the solar neutrinos are unaffected as no $\bar{\nu}'s$ are emitted in the Sun. This proposal can be tested by Mini-Boone seeing LSND effect in $\bar{\nu}_\mu$ beam, but not in the ν_μ beam, and by the fact that the ν_e and $\bar{\nu}_e$ oscillations with δm_{atm}^2 will be very different (present in former and absent in latter). For example, KamLAND¹²¹ will see no effect in reactor $\bar{\nu}'_e s$ even if LMA-MSW is the correct solution for solar $\nu'_e s$. This is of course at odds with the KamLAND confirmation of the LMA-MSW solution. At neutrino factories, (fractional) CPT violating mass differences and mixing parameters can be probed to a percent level¹¹⁹. It should be stressed that models which have different masses for particles and antiparticles only seem Lorentz invariant (and non-local); however, the neutrino propagators will also violate Lorentz invariance and so they are actually Lorentz non-invariant as well¹²².

After the announcement of KamLAND results, which are in general agreement with the expectations from LMA-MSW and hence CPT conservation; a modified CPT -violating scenario to account for LSND has been proposed¹²³. The idea is that in the anti-neutrino sector, instead of the LSND and the atmospheric splittings, now there are the LSND and the KamLAND splittings. At the moment it seems possible to fit the atmospheric data. The solar mass difference and the KamLAND mass differences need not be the same, hence LMA-MSW is not yet established according to the authors.

8.2 Lorentz Invariance Violation in Neutrino Oscillations

A general formalism to describe small departures from exact Lorentz invariance has been developed by Colladay and Kostelecky¹²⁴. This modification of Standard Model is renormalizable and preserves the gauge symmetries. When rotational invariance in a preferred frame is imposed, the formalism developed by Coleman and Glashow¹²⁵ can be used. In this form, the main effect (at high energies) of the violation of Lorentz invariance is that each particle species i has its own maximum attainable velocity (MAV), c_i , in this frame. The Lorentz violating parameters are $c_i^2 - c_j^2$. There are many interesting consequences¹²⁵: evading

of GZK cut-off, possibility of “forbidden” processes at high thresholds e.g. $\gamma \rightarrow e^+ + e^-$, $p \rightarrow e^+ + n + \nu$, $\mu \rightarrow \pi + \nu_\mu$, $\mu \rightarrow e + \gamma$ etc. Moreover, even if neutrinos were massless, the flavour eigenstates could be mixtures of velocity (MAV) eigenstates and the flavour survival probability (in the two flavour case) is given by

$$P_{\alpha\alpha} = 1 - \sin^2 2\theta \sin^2 \left(\frac{\delta c}{2} LE \right) \quad \dots (53)$$

where $\delta c = c_1 - c_2$. Identical phenomenology for neutrino oscillations arises in the case of flavour violating gravity or the violation of equivalence principle (VEP), with $\delta\gamma\Phi$ replacing δc . Here Φ is the gravitational potential and $\delta\gamma = \gamma_1 - \gamma_2$ is the difference in the post-Newtonian parameters used to test General Relativity¹²⁶ and which break the equivalence principle. This mechanism was first proposed by Gasperini and by Halprin and Leung^{127, 128}. It provides a different realization of the phenomenon of oscillation amongst massless neutrinos, first proposed in ref.[41] in the context of neutrino non-standard interactions, as discussed in Sec. 5. There are, however, some important theoretical differences between the two proposals. There does not seem to be a consistent theoretical scheme for VEP, since no theory of gravity obeying the classic General Relativity tests and also violating the equivalence principle has ever been found¹²⁹. In contrast the resonant oscillation of massless neutrinos due to NSI has a well-defined theoretical basis, either in terms of effective neutrino non-orthonormality, or due to the existence of new particles coupled to neutrinos^{41, 77}. The VEP form of massless neutrino oscillations was very interesting at one time. The reason was that a single choice of parameters δc and $\sin^2 2\theta$ could account for both atmospheric and solar neutrinos with $\nu_e - \nu_\mu$ mixing¹³⁰. However, now $\nu_\mu - \nu_e$ can no longer account for atmospheric neutrinos⁵⁴ and the LE dependence is ruled out for atmospheric neutrinos¹³¹, except as a sub-leading effect. A description of solar neutrinos, even including the recent SNO data, is still possible¹³²; with the choice of parameters: $\delta c/2 \sim 10^{-24}$ and large mixing. However, this is ruled out to the extent that KamLAND confirms the LMA-MSW solution for solar neutrinos; and hence must be a sub-leading effect. For $\nu_\mu - \nu_x$ mixing, the results of CCFR¹³³ can be used to constrain $\delta c/2 < 10^{-21}$ (for $\sin^2 2\theta > 10^{-3}$), and future Long Baseline experiments¹³⁴ will extend the bounds

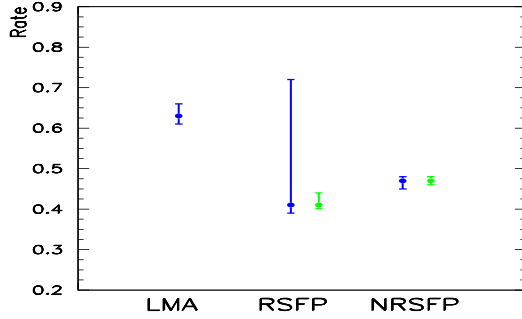


Fig. 25 Predicted R_{Borexino} values for LMA-MSW and spin flavour precession solutions, from ref.[56].

to 10^{-23} for large mixing. In the general case, when neutrinos are not massless, the energies are given by

$$E_i = p + m_i^2/2p + c_i p \quad \dots (54)$$

There will be two mixing angles (even for two flavours) and the survival probability is given by

$$P_{\alpha\alpha} = 1 - \sin^2 2\Theta \sin^2(\Delta L/4) \quad \dots (55)$$

where

$$\Delta \sin 2\Theta = | (\delta m^2/E) \sin 2\theta_m + 2\delta c e^{i\eta} E \sin 2\theta_c |, \quad \dots (56)$$

$$\Delta \cos 2\Theta = (\delta m^2/E) \cos 2\theta_m + 2\delta c E \cos 2\theta_c \dots (57)$$

One can also write the most general expression including the CPT violating term of eq.42 and even extending to three flavours. But there is not enough information to constrain the many new parameters. When data from Long Baseline experiments and eventually neutrino factories become available, CPT and Lorentz violation in neutrino oscillations can be probed to new and significant levels. It would be especially useful to have detectors capable of distinguishing between ν and $\bar{\nu}$ events.

9 Neutrino Physics with Future Experiments

9.1 Probing Spin Flavour Precession with Borexino

Irrespective of KamLAND, future data from the upcoming Borexino experiment will be useful in distinguishing the LMA-MSW solution from the spin flavour precession solutions described above in Sec. 6. Indeed, the Borexino experiment has the potential to distinguish both the NRSFP solution and the simplest RSFP solution with no mixing^{56, 135} from the

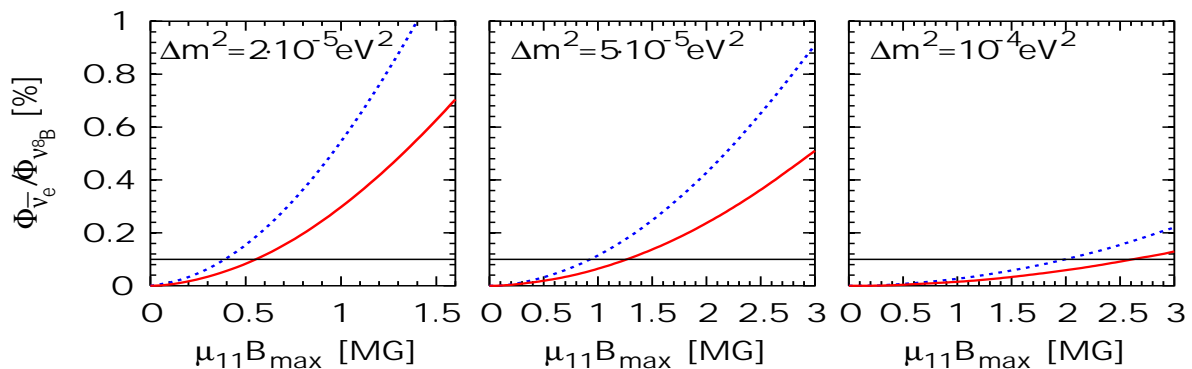


Fig. 26 KamLAND sensitivity on the Majorana neutrino transition magnetic moment for the case of the LMA-MSW solution. See text.

LMA-MSW solution, as summarized in Fig. 25. See ref.[56] for more details. On the other hand a strong confirmation of the LMA-MSW oscillation solution by KamLAND¹³⁶ would imply that spin-flavour-precession may at best be present at a sub-leading level, leading to a constraint on μB_{\perp} .

Note that, if transition magnetic moments exist, then neutrino conversions within the Sun will result in partial polarization of the initial solar neutrino fluxes. This opens a new opportunity to observe the electron antineutrinos¹³⁷. By measuring the slopes of the energy dependence of the differential neutrino electron scattering cross section one can show how $\nu_e \rightarrow \bar{\nu}_e$ conversions may take place for low energy solar neutrinos in the Borexino region, while being unobservable at the Kamiokande and Super-Kamiokande experiments.

9.2 Probing Spin Flavour Precession with KamLAND

Accepting the LMA-MSW solution to the solar neutrino anomaly, as indicated by first KamLAND results, one can still probe the admixture of alternative mechanisms of solar neutrino conversion, such as Spin Flavour Precession. In fact we argue that this will be an interesting object of study. With sufficient statistics it should be possible to constrain such sub-leading admixtures, as discussed in ref.[56]. As an illustration, one can place a constraint on μB_{\perp} (here B_{\perp} is the maximum transverse solar magnetic field at the convective zone) by searching for a solar anti-neutrino flux, expected in the SFP scenarios. This constraint depends on how good is the KamLAND determination of the LMA-MSW oscillation parameters, as illustrated in Fig. 26. In this Figure we have

displayed the electron anti-neutrino flux predicted at KamLAND ($E > 8.3$ MeV) for three different Δm_{SOL}^2 values (indicated in the figure) and for $\tan^2 \theta_{\text{SOL}}$ values varying in the range from 0.3-0.8, as a function of $\mu_{11}B_{\text{max}}$, μ_{11} being the magnetic moment in units of 10^{-11} Bohr magneton and B_{max} being the maximum magnetic field in the convective zone. The extremes of the neutrino mixing range correspond to the solid and dashed lines indicated in the figure, while the horizontal line corresponds to a KamLAND sensitivity on the anti-neutrino flux of 0.1 %, expected with three years running¹³⁶. Clearly the limits on the transition magnetic moments are sensitive also to the ultimate central Δm_{SOL}^2 value indicated by KamLAND, being more stringent for lower Δm_{SOL}^2 values, as seen from the left panel. A 10 % error on Δm_{SOL}^2 is aimed at by the collaboration.

9.3 Constraining Neutrino Magnetic Moments with Borexino

Solar neutrino data can also be used to derive stringent bounds on Majorana neutrino transition magnetic moments μ_{ij} ^{92,138}, irrespective of the value of the solar magnetic field. As discussed in ref.[139] accepting that LMA-MSW accounts for the solar neutrino data, one can still probe Majorana neutrino transition magnetic moments: if present they would contribute to the neutrino–electron scattering cross section and hence affect the signal observed in Super-Kamiokande. Assuming that LMA-MSW is the solution of the solar neutrino problem ref.[139] constrains neutrino TMs by using the latest global solar neutrino data. One finds that *all* elements of the TM matrix can be bounded at the same time. Moreover, ref.[139] shows how reactor data play a complementary role to the solar neutrino data. The resulting combined solar

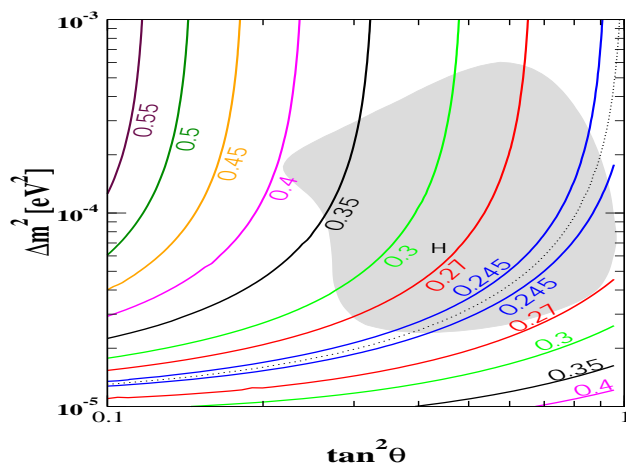


Fig. 27 Contours of the 90% C.L. bound on the magnitude of the Majorana neutrino magnetic moments after 3 years of Borexino data-taking, in units of $10^{-10}\mu_B$. The current best fit point is shown by the star, and the shaded region is the allowed LMA-MSW region at 3σ , from the first paper in ref.[139].

plus reactor bound on TMs is $2 \times 10^{-10}\mu_B$ at the 90% C.L.

Contours of the 90% C.L. bound on the magnitude of the Majorana neutrino magnetic moments after 3 years of Borexino data-taking, in units of $10^{-10}\mu_B$ are displayed in Fig. 27. In this figure the current best fit point is denoted by the star, and the shaded region is the allowed 3σ LMA-MSW region obtained in the first paper in ref.[139], where details of the analysis can be found. One sees that, thanks to the lower energy, the sensitivity of the upcoming Borexino experiment is about an order of magnitude better than that of current solar neutrino data. Given the relative delay in the start of the Borexino experiment, probing neutrino magnetic moments constitutes one of its most interesting physics goals, as no other current experiment can probe TMs with comparable sensitivity. Another interesting item for Borexino is to test for Non-Standard neutrino interactions. This possibility has been recently discussed in ref.[140].

9.4 Constraining New Gauge Bosons at Very Low Energies

Some electroweak models with extended neutral currents, such as those based on the E_6 group³⁹, lead to an increase of the $\bar{\nu} - e$ scattering cross section at low energies, typically below 100 keV¹⁴¹. It has been suggested that the search for the effects of a heavy Z'

gauge boson contribution would be feasible in an experiment with a high-activity artificial neutrino source and a large-mass detector. The neutrino flux is known to within a percent accuracy and, in contrast to the reactor neutrino case, one can reach lower neutrino energies. Both features make the proposed experiment more sensitive to extended gauge models, such as the χ model³⁹. In Fig. 28 we briefly summarize the results obtained in ref.[142] for the case for the proposed LAMA experiment, with a large NaI(Tl) detector located at the Gran Sasso underground laboratory.

One sees that, for a low enough background, the sensitivity to the Z_χ boson mass would reach 600 GeV for one year running of the experiment. These values are reasonably competitive, and in any case complementary, to the sensitivity from direct searches at the Tevatron¹⁴³, or through precision electroweak tests¹⁴⁴.

9.5 Probing Non-Standard Interactions at Neutrino Factories

The primary goal of neutrino factories is to probe the lepton mixing angle θ_{13} with much better sensitivity than possible at present and, hopefully, also the possibility of leptonic CP violation^{145, 146}. We have already discussed both the hierarchical nature of neutrino mass splittings indicated by the observed solar and atmospheric neutrino anomalies, as well as the stringent bound on θ_{13} that follows from reactor experiments Chooz and Palo Verde. We also mentioned in Sec.2.1 that the leptonic CP violation associated with the standard Dirac phase present in the simplest three-neutrino system (characterized by a unitary CC mixing matrix) disappears³⁷ as two neutrinos become degenerate and/or as $\theta_{13} \rightarrow 0$. As a result, although the large mixing indicated by current solar neutrino data certainly helps, direct leptonic CP violation tests in oscillation experiments will be a very demanding task for neutrino factories.

Here we emphasise the role of neutrino factories in probing non-standard interactions. It has been shown¹⁴⁷ that NSI in the $\nu_\mu - \nu_\tau$ channel can be studied with substantially improved sensitivity in the case of flavour changing NSI, especially at energies higher than approximately 50 GeV, as illustrated in Fig. 29. For example, a 100 GeV *Nufact* can probe FC-NSI interactions at the level of $|\epsilon| < \text{few} \times 10^{-4}$ at 99 % C.L. Note also that in such hybrid solutions to the neutrino anomalies, with FC-NSI explaining the solar data, and oscillations accounting for the atmospheric data, the

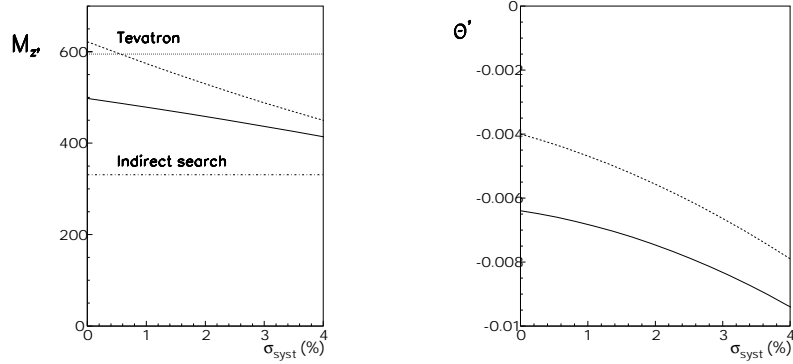


Fig. 28 Attainable 95 % C. L. sensitivity to the mass (left panel) and mixing (right) of an extra gauge boson in the χ model, plotted versus the systematic error per bin. The results correspond to the cases of a 400 kg (solid line) and 1-ton detector (dashed line).

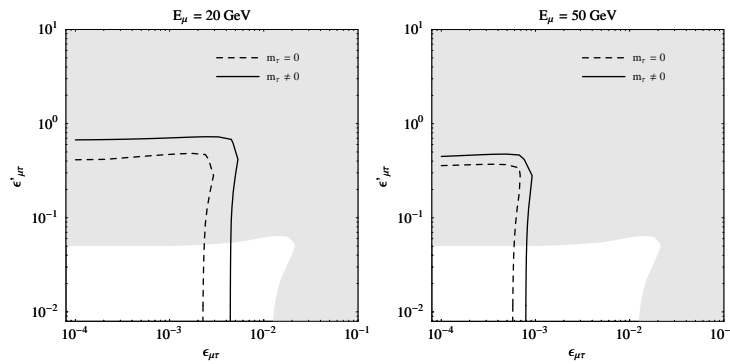


Fig. 29 Comparing the sensitivity to neutrino NSI of current atmospheric neutrino experiments (white) with future neutrino factory experiments (grey), details in ref.[147].

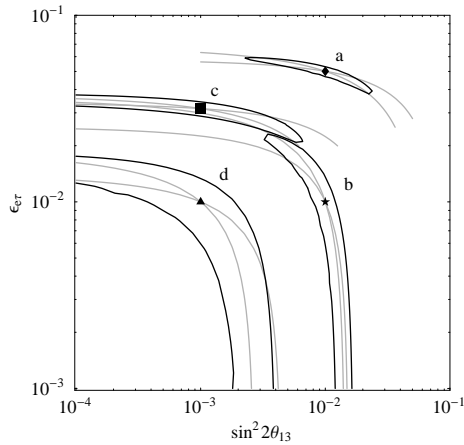


Fig. 30 99% C.L. allowed regions (black lines) in $\sin^2 2\theta_{13} - \epsilon_{e\tau}$ for different input values, as indicated by the points, at a baseline of 3000km. Lines of constant event rates are displayed in grey. Details in ref.[148].

two sectors are connected not only by the neutrino mixing angle θ_{13} , but also by the $\nu_e - \nu_\tau$ flavour changing NSI parameters. As a result NSI and oscillations may be confused, as shown in ref.[148]. This implies that information on θ_{13} can only be obtained if bounds on NSI are available. Taking into account the existing

bounds on FC interactions, one finds a drastic loss in *Nufact* sensitivities on θ_{13} , of at least two orders of magnitude, as illustrated in Fig. 30.

A near-detector offers the possibility to obtain stringent bounds on some NSI parameters and therefore constitutes a crucial necessary step towards the determination of θ_{13} and subsequent study of leptonic *CP* violation.

10 Discussion and Outlook

These are exciting times for neutrino physics, driven mainly by experiment. We have given a brief overview on the status of neutrino oscillation physics, including the determination of mass splittings and mixings from current data. Recent results bring substantial expectation on the potential of future data both of KamLAND and K2K which provide independent tests of the solar and atmospheric neutrino anomalies from terrestrial, man-controlled neutrino sources. The solar neutrino Δm_{SOL}^2 will be better determined after 3 years of KamLAND running, especially if the solar data also improve in the meantime. Unfortunately progress in the determination of the solar angle will

be less impressive. In contrast to the Cabibbo angle, the mixing between the first two generations of leptons has been shown to be large, though significantly non-maximal. This opens new ways to probe the solar interior as well as supernovae.

KamLAND has brought a turning point to the possibility of non-oscillation descriptions of the solar neutrino data, such as those invoking spin-flavor precession or non-standard neutrino interactions. Although such descriptions currently provide an excellent fit of the solar data, they are now globally disfavored by about 3σ and can only play a sub-leading role in the solar neutrino anomaly. Analysing in further detail the resulting constraints is beyond the scope of this short review, which was commissioned well before these results were available.

Accepting the LMA-MSW solution, we have nevertheless illustrated how current and future neutrino data can place important restrictions on non-standard neutrino properties, such as magnetic moments. We have also discussed the potential in constraining non-standard neutrino properties of future data from experiments such as KamLAND, Borexino and the upcoming neutrino factories.

We have also considered how solar and atmospheric neutrino data can be used to place constraints on neutrino instability, as well as *CPT* and Lorentz

Violation. Let us stress that interest still persists in the investigation of non-standard neutrino properties, to the extent that, at least some, are well-motivated by theory.

Last, but not least, non-oscillation phenomena such as neutrinoless double beta decay would, if discovered, probe the absolute scale of neutrino mass and also reveal their Majorana nature. With the era of neutrino properties entering a new age, we can only hope that the underlying mechanism for generating neutrino mass will start revealing its nature, a formidable task indeed.

Acknowledgements

This work was supported in part by Spanish grant BFM2002-00345, by the European Commission RTN grant HPRN-CT-2000-00148, by the ESF *Neutrino Astrophysics Network*, and by the U.S. D.O.E. under grant DE-FG03-91ER40833. We thank all our collaborators, for the physics and for the fun, especially those directly involved on the analysis of recent neutrino data. Special thanks also to Michele Maltoni and Timur Rashba, for technical help, to Sergio Pastor and Georg Raffelt for discussions on Sec. 4, and to Mariam Tortola for proof-reading. One of us (S.P.) would like to thank the Theory group at KEK for their hospitality while this work was carried out.

References

- 1 B T Cleveland *et al* "Measurement of the Solar Electron Neutrino Flux with the Homestake Chlorine Detector" *Astrophys J* **496** (1998) 505
- 2 W Hampel *et al* GALLEX Collaboration "GALLEX solar neutrino observations:..." *Phys Lett B* **447** (1999) 127
- 3 J N Abdurashitov *et al* SAGE Collaboration "Measurement of the solar neutrino capture rate by SAGE..." *Phys Rev Lett* **83** (1999) 4686; *Phys Rev C* **60** (1999) 055801; *J Exp Theor Phys* **95** (2002) 181; *Zh Eksp Teor Fiz* **122** (2002) 211
- 4 M Altmann *et al* GNO Collaboration "GNO solar neutrino observations..." *Phys Lett B* **490** (2000) 16; E Bellotti *Nucl Phys Proc Suppl* **91** (2001) 44
- 5 S Fukuda *et al* Super-K Collaboration "Determination of solar neutrino oscillation parameters using 1496 days..." *Phys Lett B* **539** (2002) 179 and references therein
- 6 Q R Ahmad *et al* SNO Collaboration "Direct evidence for neutrino flavor transformation from neutral-current ..." *Phys Rev Lett* **89** (2002) 011301 and "Measurement of day and night neutrino energy spectra at SNO..." *Phys Rev Lett* **89** (2002) 011302
- 7 Q R Ahmad *et al* SNO Collaboration "Measurement of the charged current interactions produced by B-8 solar neutrinos..." *Phys Rev Lett* **87** (2001) 071301
- 8 J Bahcall Int Conf. on Neutrino Physics and Astrophysics Munich 2002; B Ricci, V Berezinsky, S Degl'Innocenti, W A Dziembowski, and G Fiorentini "Helioseismic constraints to the central solar temperature and neutrino fluxes" *Phys Lett B* **407** (1997) 155
- 9 M Maltoni, T Schwetz, M A Tortola and J W F Valle "Constraining neutrino oscillation parameters with current solar and atmospheric data" hep-ph/0207227 *Phys Rev D* **67** (2003) 013011. This paper gives an extensive list of earlier references on solar neutrino data analyses
- 10 L Wolfenstein, "Neutrino Oscillations In Matter" *Phys Rev D* **17** (1978) 2369; S P Mikheev and A Y Smirnov "Resonance Enhancement of Oscillations..." *Sov J Nucl Phys* **42** (1985) 913

- 11 M C Gonzalez-Garcia *et al* "Status of the MSW solutions of the solar neutrino problem" *Nucl Phys B* **573** (2000) 3; J N Bahcall, P I Krastev and A Y Smirnov *Phys Rev D* **60** (1999) 093000
- 12 Y Fukuda *et al* Kamiokande Coll *Phys Lett B* **335** (1994) 237; R Becker-Szendy *et al* IMB Coll *Nucl Phys B* (Proc Suppl) **38** (1995) 331; W W M Allison *et al* Soudan Coll *Phys Lett B* **449** (1999) 137; Super-Kamiokande Coll Y Fukuda *et al* *Phys Rev Lett* **81** (1998) 1562 and **82** (1999) 2644; C McGrew in *Neutrino Telescopes 2001* Venice Italy March 2001; T Toshito in *Moriond 2001* Les Arcs France March 2001; M Ambrosio *et al* MACRO Coll *Phys Lett B* **434** (1998) 451; M Spurio *et al* hep-ex/0101019; B Barish Proc of *Neutrino 2000* <http://nu2000.sno.laurentian.ca>; A Surdo Talk given at *TAUP 2001* 8–12 September 2001 Gran Sasso Italy (<http://www.lngs.infn.it/>)
- 13 G Battistoni *et al* "Progresses in the validation of the FLUKA atmospheric nu flux calculations" *Nucl Phys Proc Suppl* **110** (2002) 336
- 14 A Aguilar *et al* LSND Collaboration "Evidence for neutrino oscillations..." *Phys Rev D* **64** (2001) 112007; See also talk by G Drexlin at International Conference on Neutrino Physics and Astrophysics <http://neutrino2002.ph.tum.de/pages/transparencies2.html>
- 15 Y Declais *et al* "Search for neutrino oscillations... from a nuclear power reactor at Bugey" *Nucl Phys B* **434** (1995) 503
- 16 F Dydak *et al* "A Search For Muon-Neutrino Oscillations..." *Phys Lett B* **134** (1984) 281
- 17 B Armbruster *et al* KARMEN Collaboration "Upper limits for neutrino oscillations $\bar{\nu}_\mu \rightarrow \bar{\nu}_e$..." *Phys Rev D* **65** (2002) 112001
- 18 M Apollonio *et al* CHOOZ Collaboration "Limits on neutrino oscillations from the CHOOZ experiment," *Phys Lett B* **466** (1999) 415; F Boehm *et al* Palo Verde Coll "Final results from the Palo Verde..." *Phys Rev D* **64** (2001) 112001
- 19 K Eguchi *et al* KamLAND Collaboration "First results from KamLAND Evidence for reactor anti-neutrino disappearance" *Phys Rev Lett* **90** (2003) 021802 hep-ex/0212021
- 20 M H Ahn *et al* K2K Collaboration "Indications of neutrino oscillation in a 250-km long-baseline experiment" *Phys Rev Lett* **90** (2003) 041801 hep-ex/0212007
- 21 M Gell-Mann, P Ramond and R Slansky in *Supergravity* (North Holland Amsterdam 1979); T. Yanagida in *Proc. of the Workshop on Unified Theory and Baryon Number of the Universe* KEK Japan 1979
- 22 R N Mohapatra and G Senjanovic "Neutrino Mass And Spontaneous Parity Nonconservation " *Phys Rev Lett* **44** (1980) 912; J Schechter and J W F Valle "Neutrino Masses in SU(2) \otimes U(1) Theories" *Phys Rev D* **22** (1980) 2227
- 23 Y Chikashige, R N Mohapatra and R D Peccei "Are there Real Goldstone Bosons ...?" *Phys Lett B* **98** (1981) 265; J Schechter and J W F Valle "Neutrino Decay And Spontaneous Violation Of Lepton Number" *Phys Rev D* **25** (1982) 774; G B Gelmini and J W F Valle "Fast Invisible Neutrino Decays," *Phys Lett B* **142** 181 (1984)
- 24 S Weinberg "Opening Address, Neutrinos 78" Proc West Lafayette (1978) 1; R Barbieri, J R Ellis and M K Gaillard "Neutrino Masses and Oscillations in SU(5)" *Phys Lett B* **90** (1980) 249
- 25 A Zee "A Theory Of Lepton Number Violation..." *Phys Lett B* **93** (1980) 389 Err-ibid **B 95** (1980) 461; K S Babu "Model Of 'Calculable'..." *Phys Lett B* **203** (1988) 132
- 26 A Masiero and J W Valle "A Model For Spontaneous R Parity Breaking" *Phys Lett B* **251** (1990) 273; J C Romao *et al* "How To Spontaneously Break R-Parity" *Phys Lett B* **288** (1992) 311; J C Romao and J W Valle "Neutrino Masses In Supersymmetry..." *Nucl Phys B* **381** (1992) 87; for early pre-LEP papers see C S Aulakh, R N Mohapatra *Phys Lett B* **119** (1982) 13; G G Ross, J W F Valle *Phys Lett B* **151** (1985) 375; J R Ellis *et al* *Phys Lett B* **150** (1985) 142; A Santamaria, J W F Valle *Phys Lett B* **195** 423 (1987); *Phys Rev Lett* **60** 397 (1988); *Phys Rev D* **39** 1780 (1989)
- 27 M A Diaz *et al* "Minimal supergravity with R-parity breaking" *Nucl Phys B* **524** (1998) 23; M Hirsch *et al* "Neutrino masses and mixings from supersymmetry..." *Phys Rev D* **62** (2000) 113008 Err-ibid **D 65** (2002) 119901 and references therein
- 28 M Hirsch *et al* "Probing neutrino properties with charged scalar lepton decays" *Phys Rev D* **66** (2002) 095006; W Porod *et al* "Testing neutrino mixing at future collider experiments" *Phys Rev D* **63** (2001) 115004; D Restrepo, W Porod and J W Valle "Broken R-parity stop decays and neutrino physics" *Phys Rev D* **64** (2001) 055011; S Y Choi, E J Chun, S K Kang and J S Lee "Neutrino oscillations and R-parity... signals" *Phys Rev D* **60** (1999) 075002; J C Romao *et al* "A supersymmetric solution..." *Phys Rev D* **61** (2000) 071703; B Mukhopadhyaya, S Roy and F Vissani "Correlation between neutrino oscillations..." *Phys Lett B* **443** (1998) 191
- 29 A Ioannisian and J W Valle "SO(10) grand unification model for degenerate neutrino masses" *Phys Lett B* **332** (1994) 93; D O Caldwell and R N Mohapatra "Neutrino Mass Explanations Of Solar And Atmospheric Neutrino Deficits And Hot Dark Matter" *Phys Rev D* **48** (1993) 325
- 30 K S Babu, E Ma and J W F Valle "Underlying A(4) symmetry for the neutrino mass matrix and the quark mixing matrix," *Phys Lett B* **552** (2003) 207 hep-ph/0206292
- 31 See eg P H Chankowski *et al* "Neutrino unification" *Phys Rev Lett* **86** (2001) 3488 hep-ph/0011150
- 32 S Davidson and S F King "Bi-maximal neutrino mixing in the MSSM with a single right-handed neutrino" *Phys Lett B* **445** (1998) 191; Q Shafi and Z Tavartkiladze "Bi-maximal neutrino mixings and proton decay in SO(10)..." *Phys Lett B* **487** (2000) 145; K S Babu and R N Mohapatra "Predictive schemes for bimaximal neutrino mixings" *Phys Lett B* **532** (2002) 77

- 33 For reviews see eg G Altarelli and F Feruglio “Neutrino Masses And Mixings: A Theoretical Perspective” *Phys Rept* **320** (1999) 29; S M Barr and I Dorsner “A general classification of three neutrino models...” *Nucl Phys B* **585** (2000) 79; G G Ross and L Velasco-Sevilla “Symmetries and fermion masses” hep-ph/0208218 and S King talk at Neutrino 2002
- 34 J Schechter and J W F Valle “Neutrino Masses in $SU(2) \otimes U(1)$ Theories” *Phys Rev D* **22** (1980) 2227
- 35 J Schechter and J W F Valle “Neutrino Oscillation Thought Experiment” *Phys Rev D* **23** (1981) 1666
- 36 M Doi, T Kotani, H Nishiura, K Okuda and E Takasugi “CP Violation in Majorana Neutrinos” *Phys Lett B* **102** (1981) 323. For a recent review see S M Bilenky, C Giunti and W Grimus “Phenomenology of neutrino oscillations” *Prog Part Nucl Phys* **43** (1999) 10
- 37 J Schechter, J W F Valle “Comment on The Lepton Mixing Matrix” *Phys Rev D* **21** (1980) 309
- 38 G C Branco *et al* “Leptonic CP Violation with Massless Neutrinos,” *Phys Lett B* **225** (1989) 385; N Rius, J W F Valle “Leptonic CP Violating Asymmetries...,” *Phys Lett B* **246** (1990) 249; M C Gonzalez-Garcia and J W F Valle “Enhanced lepton flavor violation with massless neutrinos...” *Mod Phys Lett A* **7** (1992) 477; A Ilakovac, A Pilaftsis *Nucl Phys B* **437** (1995) 491; J Bernabeu *et al Phys Lett B* **187** (1987) 303
- 39 For a review see J W F Valle “Gauge Theories And The Physics of Neutrino Mass” *Prog Part Nucl Phys* **26** (1991) 91
- 40 R N Mohapatra and J W F Valle “Neutrino Mass And Baryon-Number Nonconservation In Superstring Models ” *Phys Rev D* **34** (1986) 1642
- 41 J W F Valle “Resonant Oscillations of Massless Neutrinos In Matter” *Phys Lett B* **199** (1987) 432
- 42 J T Peltoniemi, D Tommasini and J W F Valle “Reconciling dark matter and solar neutrinos” *Phys Lett B* **298** (1993) 383; J T Peltoniemi and J W F Valle “Reconciling dark matter solar and atmospheric neutrinos” *Nucl Phys B* **406** (1993) 409; Caldwell and Mohapatra in ref.[29]; Giunti and Lavader’s excellent web–page <http://www.to.infn.it/~giunti/neutrino/>
- 43 M Maltoni, T Schwetz and J W F Valle “Status of four-neutrino mass schemes: A global and unified approach to current neutrino oscillation data” *Phys Rev D* **65** (2002) 093004 hep-ph 0112103
- 44 M Maltoni, T Schwetz, M A Tortola and J W F Valle “Ruling out four-neutrino oscillation interpretations of the LSND anomaly?” *Nucl Phys B* **643** (2002) 321 hep-ph/0207157
- 45 A Osipowicz *et al* KATRIN Coll, “Katrin: A next generation tritium beta decay experiment with sub-eV sensitivity for the electron neutrino mass” hep-ex/0109033 and references therein
- 46 O Elgaroy *et al* “A new limit on the total neutrino mass from the 2dF galaxy redshift survey” *Phys Rev Lett* **89** (2002) 061301 astro-ph/0204152 For a theoretical discussion see S Hannestad “Can cosmology detect hierarchical neutrino masses?,” *Phys Rev D* **67** (2003) 085017 astro-ph/0211106
- 47 K Hagiwara *et al* “Review Of Particle Physics” *Phys Rev D* **66** (2002) 010001
- 48 For reviews on double beta decay experiments and nuclear theory see A Morales *Nucl Phys Proc Suppl* **77** (1999) 335; P Vogel nucl-th/0005020; A Faessler and F Simkovic *Prog Part Nucl Phys* **46** (2001) 233; M Doi, T Kotani and E Takasugi “Double Beta Decay And Majorana Neutrino” *Prog Theor Phys Suppl* **83** (1985) 1
- 49 J Schechter and J W F Valle “Neutrinoless Double-Beta Decay In $SU(2) \times U(1)$ Theories ” *Phys Rev D* **25** (1982) 2951
- 50 L Wolfenstein “Different Varieties Of Massive Dirac Neutrinos” *Nucl Phys B* **186** (1981) 147; J W F Valle and M Singer “Lepton Number Violation with Quasi Dirac Neutrinos” *Phys Rev D* **28** (1983) 540
- 51 J W F Valle “Neutrinoless Double-Beta Decay with Quasi-Dirac Neutrinos” *Phys Rev D* **27** (1983) 1672
- 52 V Barger, S L Glashow, D Marfatia and K Whisnant “Neutrinoless double beta decay can constrain neutrino dark matter” *Phys Lett B* **532** (2002) 15; F Feruglio, A Strumia and F Vissani “Neutrino oscillations and signals in beta and $0\nu 2\beta$ experiments” *Nucl Phys B* **637** (2002) 345; H Minakata, H Sugiyama “Constraints on neutrino mixing parameters by observation of neutrinoless double beta decay” *Phys Lett B* **532** (2002) 275
- 53 H V Klapdor-Kleingrothaus *et al* GENIUS Collaboration “GENIUS: A supersensitive germanium detector system for rare events” hep-ph/9910205; E Fiorini “Cuore: A Cryogenic Underground Observatory For Rare Events” *Phys Rept* **307** (1998) 309; A Bettini “Neutrino Physics At Gran Sasso Laboratory” *Nucl Phys Proc Suppl* **100** (2001) 332
- 54 M C Gonzalez-Garcia *et al* “Global three-neutrino oscillation analysis of neutrino data” *Phys Rev D* **63** 033005 (2001) hep-ph/0009350
- 55 Talk by E Lisi at XXth International Conference on Neutrino Physics and Astrophysics <http://neutrino2002.ph.tum.de/pages/transparencies2.html> and references therein
- 56 J Barranco *et al* “Confronting spin flavor solutions of the solar neutrino problem with current and future solar neutrino data” *Phys Rev D* **66** (2002) 093009 hep-ph/0207326 v3 KamLAND updated version
- 57 N Fornengo *et al* “Probing neutrino non-standard interactions with atmospheric neutrino data” *Phys Rev D* **65** (2002) 013010 hep-ph/0108043
- 58 N Fornengo *et al* “Updated global analysis of the atmospheric neutrino data in terms of neutrino oscillations” *Nucl Phys B* **580** (2000) 58 hep-ph/0002147
- 59 M Maltoni, T Schwetz and J W F Valle “Combining first KamLAND results with solar neutrino data” *Phys Rev D* **67** (2003) 093003 hep-ph/0212129
- 60 P Vogel and J Engel “Neutrino Electromagnetic Form-Factors” *Phys Rev D* **39** (1989) 3378

- 61 H Murayama and A Pierce “Energy spectra of reactor neutrinos at KamLAND” *Phys Rev D* **65** (2002) 013012
- 62 The KamLAND proposal, Stanford-HEP-98-03; A Piepke talk at *Neutrino-2000* XIXth International Conference on Neutrino Physics and Astrophysics Sudbury Canada June 2000
- 63 P Vogel and J F Beacom “The angular distribution of the reaction $\bar{\nu}_e + p \rightarrow e^+ + n$ ” *Phys Rev D* **60** (1999) 053003
- 64 E D Church, K Eitel, G B Mills and M Steidl “Statistical analysis of different $\bar{\nu}_\mu \rightarrow \bar{\nu}_e$ searches” *Phys Rev D* **66** (2002) 013001
- 65 P C de Holanda and A Smirnov *JCAP* **0302** (2003) 001 hep-ph/0212270; P Aliani *et al* hep-ph/0212212; H Nunokawa, W J Teves and R Z Funchal *Phys Lett B* **562** (2003) 28 hep-ph/0212202; J N Bahcall, M C Gonzalez-Garcia and C Pena-Garay *JHEP* **0302** (2003) 009 hep-ph/0212147; A Bandyopadhyay, S Choubey, R Gandhi, S Goswami and D P Roy *Phys Lett B* **559** (2003) 121 hep-ph/0212146; G L Fogli, E Lisi, A Marrone, D Montanino, A Palazzo and A M Rotunno *Phys Rev D* **67** (2003) 073002 hep-ph/0212127; V Barger and D Marfatia *Phys Lett B* **555** (2003) 144 hep-ph/0212126; H Minakata and H Sugiyama *Phys Lett B* **567** (2003) 305 hep-ph/0212240
- 66 A de Gouvea and C Pena-Garay “Solving the solar neutrino...” *Phys Rev D* **64** (2001) 113011
- 67 V D Barger, D Marfatia and B P Wood “Resolving the solar neutrino problem with KamLAND” *Phys Lett B* **498** (2001) 53
- 68 A D Dolgov “Neutrinos in cosmology,” *Phys Rept* **370** (2002) 333; G G Raffelt “Astrophysical and cosmological neutrinos” hep-ph/0208024. These papers give extensive references
- 69 A D Dolgov, S H Hansen, S Pastor, S T Petcov, G G Raffelt and D V Semikoz “Cosmological bounds on neutrino degeneracy improved by flavor oscillations” *Nucl Phys B* **632** (2002) 363
- 70 E Lisi, S Sarkar and F L Villante “The big bang nucleosynthesis limit on N_ν ” *Phys Rev D* **59** (1999) 123520
- 71 C Burgess *et al* “Large mixing angle oscillations as a probe of the deep solar interior” *Astrophys J* **588** (2003) L65 hep-ph/0209094; H Nunokawa *et al* “The effect of random matter density perturbations...” *Nucl Phys B* **472** (1996) 495; A B Balantekin, J M Fetter and F N Loreti “The MSW effect in a fluctuating matter density” *Phys Rev D* **54** (1996) 3941; P Bamert, C P Burgess and D Michaud “Neutrino propagation through helioseismic waves” *Nucl Phys B* **513** (1998) 319
- 72 M T Keil, G G Raffelt and H T Janka “Monte Carlo study of supernova neutrino spectra formation” *Astrophys J* **590** (2003) 971
astro-ph/0208035
- 73 A Y Smirnov, D N Spergel and J N Bahcall “Is Large Lepton Mixing Excluded?,” *Phys Rev D* **49** (1994) 1389; B Jegerlehner, F Neubig and G Raffelt *Phys Rev D* **54** (1996) 1194; M Kachelriess, R Tomas and J W F Valle “Large lepton mixing and supernova 1987A” *JHEP* **0101** (2001) 030
- 74 M Kachelriess *et al* “SN1987A and the status of oscillation solutions to the solar neutrino problem” *Phys Rev D* **65** (2002) 073016 hep-ph/0108100
- 75 H. Minakata *et al* “Probing supernova physics with neutrino oscillations,” *Phys Lett B* **542** (2002) 239 hep-ph/0112160
- 76 G G Raffelt private communication
- 77 H Nunokawa *et al* “Resonant conversion of massless neutrinos in supernovae” *Phys Rev D* **54** (1996) 4356; H Nunokawa *et al* “Supernova bounds on supersymmetric R-parity violating interactions” *Nucl Phys B* **482** (1996) 481; D Grasso *et al* “Pulsar velocities without neutrino mass” *Phys Rev Lett* **81** (1998) 2412
- 78 G L Fogli, E Lisi, A Mirizzi and D Montanino “Revisiting nonstandard interaction effects on supernova neutrino flavor oscillations” *Phys Rev D* **66** (2002) 013009 and papers therein
- 79 M Kachelriess, R Tomas and J W F Valle “Supernova bounds on majoron-emitting decays of light neutrinos” *Phys Rev D* **62** (2000) 023004 hep-ph/0001039 See also Y Farzan “Bounds on the coupling of the majoron to light neutrinos from supernova cooling” *Phys Rev D* **67** (2003) 073015 hep-ph/0211375
- 80 L J Hall and M Suzuki “Explicit R Parity Breaking In Supersymmetric Models” *Nucl Phys B* **231** (1984) 419; For a recent review see B Allanach *et al* “Searching for R-parity violation at Run-II of the Tevatron” hep-ph/9906224
- 81 L J Hall, V A Kostelecky and S Raby “New Flavor Violations In Supergravity Models,” *Nucl Phys B* **267** (1986) 415 R Barbieri, L J Hall and A Strumia “Violations of lepton flavor and CP...” *Nucl Phys B* **445** (1995) 219; F Gabbiani, E Gabrielli, A Masiero and L Silvestrini “A complete analysis of FCNC and CP...” *Nucl Phys B* **477** (1996) 321
- 82 M Guzzo *et al* “Status of a hybrid three-neutrino interpretation of neutrino data” *Nucl Phys B* **629** (2002) 479 hep-ph/0112310 For early Refs. see refs.[10,41], and also M M Guzzo, A Masiero and S T Petcov “On the MSW effect with massless...” *Phys Lett B* **260** (1991) 15 and E Roulet, “Mikheyev-Smirnov-Wolfenstein effect with flavor-changing...” *Phys Rev D* **44** (1991) 935
- 83 M C Gonzalez-Garcia *et al* “Atmospheric neutrino observations and flavor changing interactions” *Phys Rev Lett* **82** (1999) 3202; N Fornengo *et al* *JHEP* **0007** (2000) 006
- 84 K Fujikawa and R Shrock “The Magnetic Moment Of A Massive Neutrino And Neutrino Spin Rotation” *Phys Rev Lett* **45** (1980) 963
- 85 A I Derbin *et al* “Experiment On Anti-Neutrino Scattering by Electrons...” *JETP Lett* **57** (1993) 768; also *Pisma Zh Eksp Teor Fiz* **57** (1993) 755; A V Derbin “Restriction On The Magnetic Dipole Moment Of Reactor Neutrinos” *Phys Atom Nucl* **57** (1994) 222; also *Yad Fiz* **57** (1994) 236

- 86 H B Li et al Texono Collaboration "New limits on neutrino magnetic moments..." *Phys Rev Lett* **90** (2003) 131802 hep-ex/0212003
- 87 C Brogгинi MUNU Collaboration "Preliminary Results And Status Of The Munu Experiment" *Nucl Phys Proc Suppl* **100** (2001) 267; J Vuilleumier Talk at Neutrino 2002 Munich <http://neutrino2002.ph.tum.de/>
- 88 L B Auerbach et al LSND Collaboration "Measurement of ν_e electron elastic scattering" *Phys Rev D* **63** (2001) 112001
- 89 R Schwienhorst et al DONUT Collaboration "A new upper limit for the tau-neutrino magnetic moment" *Phys Lett B* **513** (2001) 23
- 90 G G Raffelt "Limits On Neutrino Electromagnetic Properties: An Update" *Phys Rept* **320** (1999) 319
- 91 B S Neganov et al "Status of the experiment on the laboratory search for the electron antineutrino magnetic moment..." *Phys Atom Nucl* **64** (2001) 1948 *Yad Fiz* **64** (2001) 2033
- 92 J Schechter and J W F Valle "Majorana Neutrinos And Magnetic Fields" *Phys Rev D* **24** 1883 (1981) *Err-ibid D* **25** 283 (1982)
- 93 A Cisneros "Effect Of Neutrino Magnetic Moment On Solar Neutrino Observations" *Astrophys Space Sci* **10** (1971) 87; L B Okun, M B Voloshin and M I Vysotsky "Electromagnetic Properties Of Neutrino And Possible Semiannual Variation Of The Solar Neutrino Flux" *Sov J Nucl Phys* **44** (1986) 440
- 94 G Raffelt "Stars as Laboratories for Fundamental Physics" University of Chicago Press (1996)
- 95 E K Akhmedov *Phys Lett B* **213** (1988) 64; C S Lim and W J Marciano "Resonant Spin-Flavor Precession Of Solar And Supernova Neutrinos" *Phys Rev D* **37** (1988) 1368
- 96 O G Miranda et al "The simplest resonant spin-flavour solution to the solar neutrino problem" *Nucl Phys B* **595** (2001) 360
- 97 O G Miranda et al "A non-resonant dark-side solution to the solar neutrino problem" *Phys Lett B* **521** 299 (2001) hep-ph/0108145
- 98 J Schechter and J W F Valle "Neutrino Decay And Spontaneous Violation Of Lepton Number" *Phys Rev D* **25** (1982) 774
- 99 P B Pal and L Wolfenstein "Radiative Decays Of Massive Neutrinos" *Phys Rev D* **25** (1982) 766; S Petcov *Sov J Nucl Phys* **24** (1977) 340; W Marciano and A Sanda *Phys Lett B* **67** (1977) 303
- 100 J M Frere, R B Nevzorov and M I Vysotsky "Stimulated neutrino conversion and bounds on neutrino magnetic moments" *Phys Lett B* **394** (1997) 127
- 101 M C Gonzalez-Garcia and J W F Valle "Fast Decaying Neutrinos And Observable Flavor Violation In A New Class Of Majoron Models" *Phys Lett B* **216** (1989) 360
- 102 B W Lee and R E Shrock "Natural Suppression Of Symmetry Violation In Gauge Theories: Muon - Lepton And Electron Lepton Number Nonconservation," *Phys Rev D* **16** (1977) 1444
- 103 A D Dolgov et al "Primordial nucleosynthesis, majorons..." *Nucl Phys B* **496** (1997) 24 hep-ph/9610507
- 104 J W F Valle "Fast Neutrino Decay In Horizontal Majoron Models" *Phys Lett B* **131** (1983) 87
- 105 G B Gelmini, S Nussinov and T Yanagida "Does Nature Like Nambu-Goldstone Bosons?" *Nucl Phys B* **219** (1983) 31
- 106 A Jodidio et al "Search For Right-Handed Currents In Muon Decay" *Phys Rev D* **34** (1986) 1967 *Err-ibid D* **37** (1988) 237
- 107 V D Barger, W Y Keung and S Pakvasa "Majoron Emission By Neutrinos" *Phys Rev D* **25** (1982) 907
- 108 Z G Berezhiani et al "Observable Majoron emission in neutrinoless double beta decay" *Phys Lett B* **291** (1992) 99 hep-ph/9207209
- 109 S Pakvasa and K Tennakone "Neutrinos Of Non-Zero Rest Mass" *Phys Rev Lett* **28** (1972) 1415; J N Bahcall, N Cabibbo and A Yahil "Are Neutrinos Stable Particles?" *Phys Rev Lett* **28** (1972) 316; J N Bahcall et al "Tests Of Neutrino Stability" *Phys Lett B* **181** (1986) 369
- 110 A Bandyopadhyay, S Choubey and S Goswami "Neutrino decay confronts the SNO data" *Phys Lett B* **555** (2003) 33 hep-ph/0204173; A S Joshipura, E Masso and S Mohanty "Constraints on decay plus oscillation solutions..." *Phys Rev D* **66** (2002) 113008
- 111 P Lipari and M Lusignoli *Phys Rev D* **60** (1999) 013003; G Fogli et al *Phys Rev D* **59** (1999) 117303; S Choubey and S Goswami *Astropart Phys* **14** (2000) 67
- 112 V D Barger, J G Learned, P Lipari, M Lusignoli, S Pakvasa and T J Weiler, *Phys Lett B* **462** (1999) 109
- 113 J F Beacom and N F Bell "Do solar neutrinos decay?" *Phys Rev D* **65** (2002) 113009
- 114 J F Beacom, N F Bell, D Hooper, S Pakvasa and T J Weiler "Decay of high-energy astrophysical neutrinos" *Phys Rev Lett* **90** (2003) 181301 hep-ph/0211305
- 115 N Cabibbo *Phys Lett B* **72** (1978) 333; S Pakvasa *Proc of the XXth Int. Conference on High Energy Physics* ed by L Durand and L G Pondrom, AIP Conf Proc No 68 (New York 1981), Vol 2 p 1164; V Barger, K Whisnant and R N Phillips *Phys Rev Lett* **45** (1980) 2084
- 116 D Colladay and V A Kostelecky "CPT violation and the standard model" *Phys Rev D* **55** (1997) 6760
- 117 S R Coleman and S L Glashow "High-energy tests of Lorentz invariance" *Phys Rev D* **59** (1999) 116008
- 118 V D Barger, S Pakvasa, T J Weiler and K Whisnant *Phys Rev Lett* **85** (2000) 5055

- 119 S M Bilenky, M Freund, M Lindner, T Ohlsson and W Winter "Tests of CPT invariance at neutrino factories" *Phys Rev D* **65** (2002) 073024
- 120 H Murayama and T Yanagida "LSND SN1987A and CPT violation" *Phys Lett B* **520** (2001) 263; G Barenboim, L Borissov, J Lykken and A Y Smirnov "Neutrinos as the messengers of CPT violation" *JHEP* **0210** (2002) 001
- 121 A Suzuki *8th International Workshop on Neutrino Telescopes* Venice Feb 23–26 1999 Ed M Baldo-Ceolin Vol I p 325
- 122 O W Greenberg "CPT violation implies violation of Lorentz invariance" *Phys Rev Lett* **89** (2002) 231602
- 123 G Barenboim, L Borissov and J Lykken "CPT violating neutrinos in the light of KamLAND" hep-ph/0212116
- 124 D Colladay and V A Kostelecky "Lorentz-violating extension of the standard model" *Phys Rev D* **58** (1998) 116002
- 125 S R Coleman and S L Glashow "Cosmic ray and neutrino tests of special relativity" *Phys Lett B* **405** (1997) 249 hep-ph/9703240
- 126 See eg C W Misner, K S Thorne and J A Wheeler "Gravitation" W H Freeman San Francisco 1973; or S Weinberg "Gravitation and Cosmology: Principles and Applications of the General Theory of Relativity" John Wiley and Sons ISBN: 0471925675
- 127 M Gasperini "Testing The Principle Of Equivalence With Neutrino Oscillations" *Phys Rev D* **38** (1988) 2635
- 128 A Halprin and C N Leung "Can the sun shed light on neutrino gravitational interactions?" *Phys Rev Lett* **67** (1991) 1833
- 129 A Halprin, C N Leung and J Pantaleone "A Possible Violation of the Equivalence Principle by Neutrinos" *Phys Rev D* **53** (1996) 5365
- 130 J Pantaleone, A Halprin and C N Leung "Neutrino Mixing Due to a Violation of the Equivalence Principle" *Phys Rev D* **47** (1993) 4199; J N Bahcall, P I Krastev and C N Leung "Solar neutrinos and the principle of equivalence" *Phys Rev D* **52** (1995) 1770; H Minakata and H Nunokawa, "Testing the principle of equivalence by solar neutrinos" *Phys Rev D* **51** (1995) 6625
- 131 J.G. Learned, *Current Aspects of Neutrino Physics* Ed D Caldwell Springer-Verlag (2001) hep-ex/0107056; P Lipari and M Lusignoli "On exotic solutions of the atmospheric neutrino problem" *Phys Rev D* **60** 013003 (1999); G L Fogli, E Lisi, A Marrone and G Scioscia "Testing violations of special and general relativity..." *Phys Rev D* **60** (1999) 053006
- 132 A Raychaudhuri and A Sil "Violation of the equivalence principle in the light of the SNO..." *Phys Rev D* **65** 073035 (2002); A M Gago, H Nunokawa and R Zukanovich Funchal "The solar neutrino problem and gravitationally induced..." *Phys Rev Lett* **84** (2000) 4035
- 133 D Naples *et al* CCFR/NuTeV Collaboration "A high statistics search for $\nu_e (\bar{\nu}_e) \rightarrow \nu_\tau (\bar{\nu}_\tau)$ oscillations" *Phys Rev D* **59** (1999) 031101 and *Phys Rev Lett* **78** (1997) 2912
- 134 MINOS Collaboration NUMI-2-375 Report (1998); NGS Report CERN 98-02 INFN/AE-98-05 (1998). For the range accessible to neutrino factories see A Datta *Phys Lett B* **504** (2001) 247
- 135 E K Akhmedov and J Pulido *Phys Lett B* **529** (2002) 193 and *Phys Lett B* **553** (2003) 7
- 136 Talk by J Shirai at <http://neutrino2002.ph.tum.de/pages/transparencies2.html>
- 137 S Pastor *et al* "Low-energy anti-neutrinos from the sun" *Phys Lett B* **423** (1998) 118
- 138 B Kayser "Majorana Neutrinos and their Electromagnetic Properties" *Phys Rev D* **26** (1982) 1662; J F Nieves "Electromagnetic Properties of Majorana Neutrinos" *Phys Rev D* **26** (1982) 3152
- 139 W Grimus *et al* "Constraining Majorana neutrino electromagnetic properties from the LMA-MSW solution of the solar neutrino problem," *Nucl Phys B* **648** (2003) 376 hep-ph/0208132; J F Beacom and P Vogel "Neutrino magnetic moments..." *Phys Rev Lett* **83** (1999) 5222
- 140 Z Berezhiani, R S Raghavan and A Rossi "Probing non-standard couplings of neutrinos at the Borexino detector" *Nucl Phys B* **638** (2002) 62
- 141 O G Miranda, V Semikoz and J W F Valle "Neutrino electron scattering and electroweak gauge structure: Future tests" *Phys Rev D* **58** (1998) 013007 hep-ph/9712215
- 142 I Barabanov *et al* "Testing for new physics with low-energy anti-neutrino sources: LAMA as a case study" *Nucl Phys B* **546** (1999) 19 hep-ph/9808297
- 143 F Abe *et al* CDF Collaboration "Search for new gauge bosons decaying into dileptons in $p\bar{p}$ collisions at $\sqrt{s} = 1.8 - TeV$ " *Phys Rev Lett* **79** (1997) 2192
- 144 M C Gonzalez-Garcia and J W F Valle "Neutral Current And Lep Constraints On An Extra E(6) Neutral Gauge Boson: A Global Fit To Electroweak Parameters" *Phys Lett B* **259** (1991) 365. For a recent update see J Erler and P Langacker in ref.[47].
- 145 M Apollonio *et al* "Oscillation physics with a neutrino factory" hep-ph/0210192; C Albright *et al* "Physics at a neutrino factory" hep-ex/0008064. These contain an extensive list of references
- 146 M Freund, P Huber and M Lindner *Nucl Phys B* **615** (2001) 331; A Cervera, A Donini, M B Gavela, J J Gomez Cadenas, P Hernandez, O Mena and S Rigolin *Nucl Phys B* **579** (2000) 17 *Err-ibid B* **593** (2001) 731; A De Rujula, M B Gavela and P Hernandez *Nucl Phys B* **547** (1999) 2
- 147 P Huber and J W F Valle "Non-standard interactions: Atmospheric versus neutrino factory experiments" *Phys Lett B* **523** (2001) 151
- 148 P Huber, T Schwetz and J W F Valle *Phys Rev Lett* **88** (2002) 101804 hep-ph 0111224 and *Phys Rev D* **66** (2002) 013006 hep-ph 0202048